Mesoproterozoic tectonothermal development of southwestern Sweden: New age constraints using field relationships and U-Pb geochronology

by

Catherine Anne Christoffel, B.A.

Thesis

Presented to the Faculty of the Graduate School of
The University of Texas at Austin
in Partial Fulfillment
of the Requirements
for the Degree of
Master of Science in Geological Sciences

The University of Texas at Austin
December 1997

Mesoproterozoic tectonothermal development of southwestern Sweden: New age constraints using field relationships and U-Pb geochronology

Approved by
Supervising Committee:

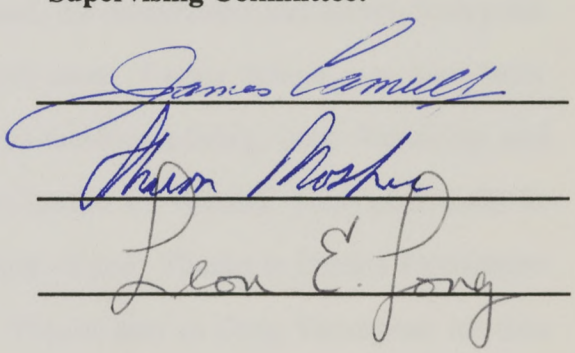

Dedication

To my parents, for their endless love and support.

Acknowledgements

I am extremely grateful to my supervisor, Jim Connelly, whose guidance, patience, wealth of knowledge, optimistic outlook, extraordinary teaching and friendship have been invaluable to me in this experience. Thanks to committee member Sharon Mosher for helpful discussions, a great experience in Structural Petrology and for valuable comments during editing. Thanks also to my other committee member, Leon Long, for introducing me to isotopes and for painstakingly thorough editing. This thesis benefited greatly from the scientific input and logistical help of Karl-Inge Åhäll, University of Göteborg, Sweden. Our discussions always proved stimulating. Tack! Kathy Manser, what would I have done without you? Your time, patience and assistance through every step of the analytical work is so appreciated, not to mention the laughter and friendship (and food). Thank you, Benjamin Pursell, for your brains and brawn during the seven weeks in Sweden and for so much more. Laurie Schuur, you have been here for it all! Thank you for your tremendous editing, your friendship and especially for all that fun! To Sven Larson of Wastad, your generosity is unsurpassed, and I smile every time I think of you. Thanks to Dennis Trombatore for being the greatest librarian ever. Thanks also to Greg Thompson for thin sections and to Lu Xianfong for help on the probe and the SEM. I appreciate computer and graphics support from Kurt Bartelmehs and Jeffrey Horowitz.

Discussions with Steve Grimes, Dave Hirsch, Rob Reed, Alex Riter and Jim Rougvie are truly appreciated. Thanks to the Department of Geological Sciences for providing five semesters and two summers of T.A. support and to the Department and to Laura and Thomas Barrow for two semesters of fellowship support. Thanks to Dr. Jim Connelly for R.A. support during summer 1996, funded by NSF Grant EAR-9418236. Thanks also to Conoco for scholarship support during my last semester. The field component of this research was made possible by grant support from the Geological Society of America, Sigma Xi, The University of Texas at Austin Geology Foundation and the Swedish Geological Survey. And to Mom and Dad, Granny, Martin and Maureen: your love, encouragement and interest in everything I do means the world to me.

Submitted to the Committee November, 1997

Abstract

Mesoproterozoic tectonothermal development of southwestern Sweden: New age constraints using field relationships and U-Pb geochronology

Catherine Anne Christoffel, MSGeoSci
The University of Texas at Austin, 1997

Supervisor: James N. Connelly

The Ätran terrane of southwestern Sweden is a Mesoproterozoic, polydeformed terrane and a product of crustal growth westward away from an Archean core. Both Gothian (Labradorian) and Sveconorwegian (Grenvillian) deformations are recorded, but it is difficult to identify the effects of each deformation because the resultant fabrics are essentially parallel. Recent debate regarding the timing of regional gneiss-formation revolves around two distinct hypotheses; one assigns the bulk of the deformation to the Gothian Orogeny and the other attributes it to the Sveconorwegian Orogeny.

U-Pb ages from four lithotectonic units constrain the timing of tectonic and thermal events for the region. Primary, igneous zircons from a felsic orthogneiss yield a protolith crystallization age of 1664±7 Ma. The first dyke suite intruded the gneisses immediately after the earliest deformation and was then metamorphosed at 1654±9 Ma during the second major deformation and migmatization event. Migmatitic layers in the gneisses and mafic dykes are cross-cut by less deformed dykes of the second dyke suite that crystallized between 1426+9/-4 Ma and 1399+7/-6 Ma. The Gothian Orogeny was thus responsible for the majority of the deformation and migmatization recorded in the study area. In addition to *ca.* 1.4 Ga magmatism, metamorphism at 1438+12/-8 Ma resulted in new zircon growth in the mafic gneiss. This magmatism and metamorphism are interpreted to be a local manifestation of a regional inter-orogenic thermal event that may be related to *ca.* 1.4 Ga magmatism known elsewhere in southwestern Sweden. Sveconorwegian deformation, constrained by the undeformed third dyke suite, occurred before 946+6/-4 Ma. Metamorphic (re)crystallization of monazite (948±9 Ma), titanite (932±5 Ma and 935±7 Ma) and rutile (878±9 Ma) indicate late-Sveconorwegian static metamorphism and suggest slow cooling rates of 4.5-11°C/million years from 948 Ma to 932 Ma and 2.5°-5°C/million years from 932 Ma to 878 Ma during erosion and collapse of the Sveconorwegian Orogen.

Table of Contents

List of Tables

List of Figures

Prologue

This thesis is divided into two chapters. Chapter 1 introduces the study, discusses project logistics and provides detailed descriptions of lithologic units in the study area and their relative structural relationships. The lithologic descriptions provide detail of mineralogical and structural aspects of the units, both macroscopic and microscopic, and may be useful for future studies of a similar nature in southwestern Sweden. Chapter 2 is a paper on the tectonothermal evolution of southwestern Sweden to be submitted to *Precambrian Research* for publication. Some material presented in Chapter 1 may be repeated in Chapter 2 because the latter is meant to stand alone.

Chapter 1: Introduction

The Grenville Orogen of North America spans the southern and eastern margins of Laurentia from Mexico, through Texas to eastern Labrador, Canada, and has been correlated across the present-day Atlantic Ocean into Scandinavia (Gower, 1990) where it is referred to as the Sveconorwegian Orogen. The relationship between these two orogenic belts is complicated because formerly interposed crustal material is now missing. Detailed studies of the Sveconorwegian Orogen that incorporate field and structural geology with reliable radiometric ages are essential to develop a better understanding of the tectonic evolution of the Baltic craton. They also facilitate correlations of tectonic and thermal events between Baltica and Laurentia.

The field area for this study is located in southwestern Sweden between Falkenberg and Halmstad (Figures 1.1 & 1.2). It was chosen for its excellent exposure and presence of structural fabrics that are similar to those of other areas in the same tectonic terrane. At least two Mesoproterozoic orogenic events affected the area; thus, accurate tectonothermal models require the correct separation of deformational and metamorphic effects into their respective orogenic events.

Discrepancies exist regarding the timing of regional gneiss-formation of the orthogneisses of southwestern Sweden (Åhäll, 1996; Connelly & Åhäll, 1996; Connelly et al., 1996; Johansson et al., 1996; Åhäll et al., 1997b; Möller &

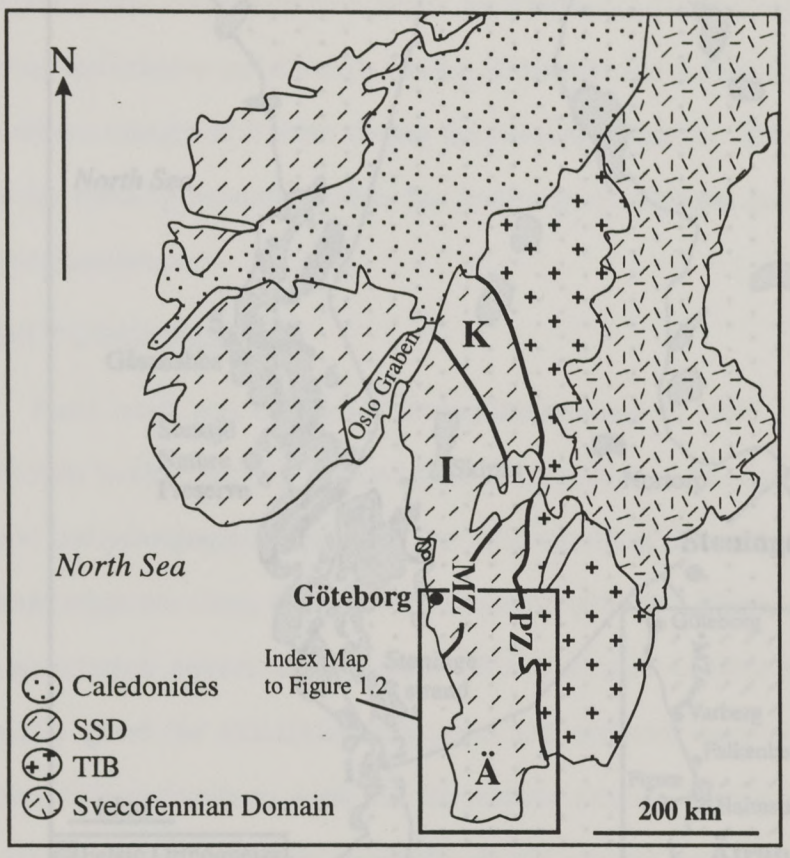

Figure 1.1. Lithotectonic terrane map of southern Scandinavia, after Connelly et al. (1996). SSD, Southwest Scandinavian Domain; TIB, Transscandinavian Igneous Belt; Ä, Ätran terrane; K, Klarälven terrane; I, Idefjorden terrane; MZ, Mylonite Zone; PZ, Protogine Zone; LV, Lake Vänern. The MZ and PZ are delineated by bold lines.

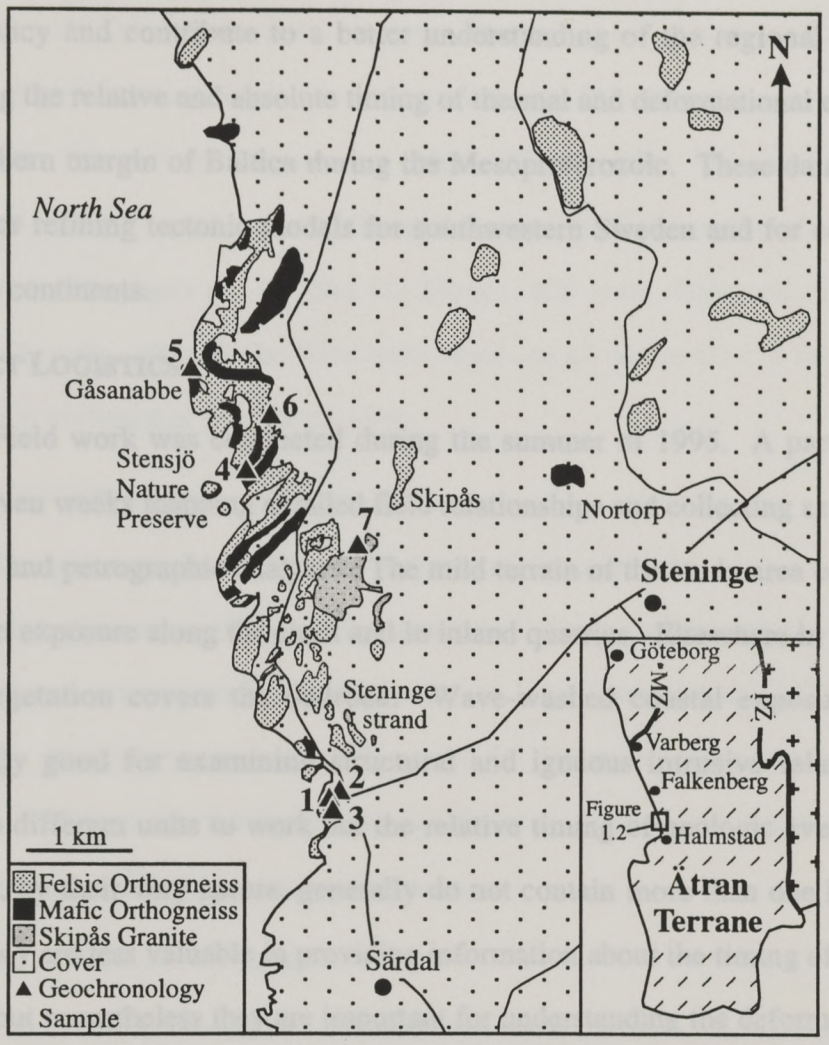

Figure 1.2. Geological map of the study area. Location of geochronological samples 1-7 indicated with solid triangles. Map redrawn from Caldenius et al. (1966) with additions and modifications from the present study. Area of inset shown on Figure 1.1.

Söderlund, 1997). New field and U-Pb data presented here address this discrepancy and contribute to a better understanding of the regional geology, including the relative and absolute timing of thermal and deformational events for the southern margin of Baltica during the Mesoproterozoic. These data are also useful for refining tectonic models for southwestern Sweden and for correlation between continents.

PROJECT LOGISTICS

Field work was conducted during the summer of 1995. A party of two spent seven weeks mapping detailed field relationships and collecting samples for isotopic and petrographic analyses. The mild terrain of the study area consists of excellent exposure along the coast and in inland quarries. Elsewhere in the study area, vegetation covers the bedrock. Wave-washed coastal exposures were especially good for examining structural and igneous intrusive relationships between different units to work out the relative timing of geologic events. The quarries, by their very nature, generally do not contain more than one lithology. Thus, they are less valuable in providing information about the timing of regional events, but nevertheless they are important for understanding the deformation and thermal history of the dominant units of the area. Sample processing and U-Pb isotopic analyses were performed at the University of Texas at Austin.

LITHOLOGIES AND STRUCTURAL RELATIONSHIPS

Four major rock units in the study area were examined to better understand their relative chronologic relationships, deformational histories and metamorphic evolution. Each unit is separated from the next youngest by one or more

deformation events (Table 1.1). Thus, the units were identified on the basis of penetrative D1-D5 deformation features. The region of interest predominantly comprises gneisses that were first deformed during D1 and were intruded by at least three generations of younger dykes (Figure 1.3). The earliest suite comprises mafic dykes that were deformed during D2. Felsic and mafic dykes of the second suite cross-cut D1 and D2 fabrics, and were deformed during D4. Felsic and mafic dykes of the third suite cross-cut all of the D1-D4 fabrics, and some show evidence of D5 deformation.

Gneiss Package

The oldest rocks in the area include interlayered felsic, intermediate and mafic orthogneisses and supracrustal gneisses. Contacts between the different orthogneisses are concordant and parallel to intra-formational S1/S2 gneissic layering. A well-developed S1/S2 composite foliation, closed to isoclinally folded (F3) foliations, L4 lineations and later, open F5 folds demonstrate the polydeformational history of the orthogneisses.

Felsic & Intermediate Orthogneisses

Felsic and intermediate orthogneisses comprise the dominant unit. The appearance of these rocks is consistent throughout the field area in both coastal and quarry exposures with the exception of the area near Skipås (Figure 1.2), discussed below. The foliation varies in intensity and is generally defined by compositional interlayers of granitic and mafic material and locally defined by weakly aligned biotite, hornblende, feldspar augen and quartz ribbons.

Table 1.1. Mesoproterozoic emplacement and deformation history in the Falkenberg-Halmstad area, southwestern Sweden. U-Pb ages from this study constrain the timing of events.

INTRUSION/ DEFORMATION (D)	ASSOCIATED FOLIATIONS (S)	ASSOCIATED FOLDS (F) & LINEATIONS (L)	AGE CONSTRAINTS
Orthogneisses (and Skipås granite)			**1664±7 Ma**
D1	**S1**, defined by **N1** leucosome	-	
1st Dyke Suite			
D2	**N2** generated & flattened. **N2** cross-cuts **N1**. **S2** parallel to **S1**.	-	**1654±9 Ma**
D3	**S3**, axial planar fabric to **F3** folds. Some minerals of **S1** & **S2** realigned.	**F3**, folds **S1** & **S2**	timing unknown. Gothian or early "Hallandian."
2nd Dyke Suite			**1426+9/-4 Ma** **1399+7/-6 Ma**
D4	**S4**	**F4** folds C-dykes, **L4**	timing poorly constrained.
D5		**F5**, gentle N-S trending	
3rd Dyke Suite (deformed)			
3rd Dyke Suite (undeformed)			**946+6/-4 Ma**

Two distinct leucosomes occur in these gneisses. The first generation (N1) consists of fine- to medium-grained, homogeneous, 0.5 to 2 cm thick, pink, gray and white layers that, in conjunction with the more mafic layers, define the S1 gneissocity (Table 1.1). Younger, medium-grained to pegmatitic leucosomes (N2) (Figure 1.4) cross-cut S1. N2 leucosomes commonly pinch out and range in thickness from 1 to 10 cm. They contain a fabric (S2) that is parallel to sub-parallel to the regional S1 foliation, thus defining a composite foliation (S1/S2).

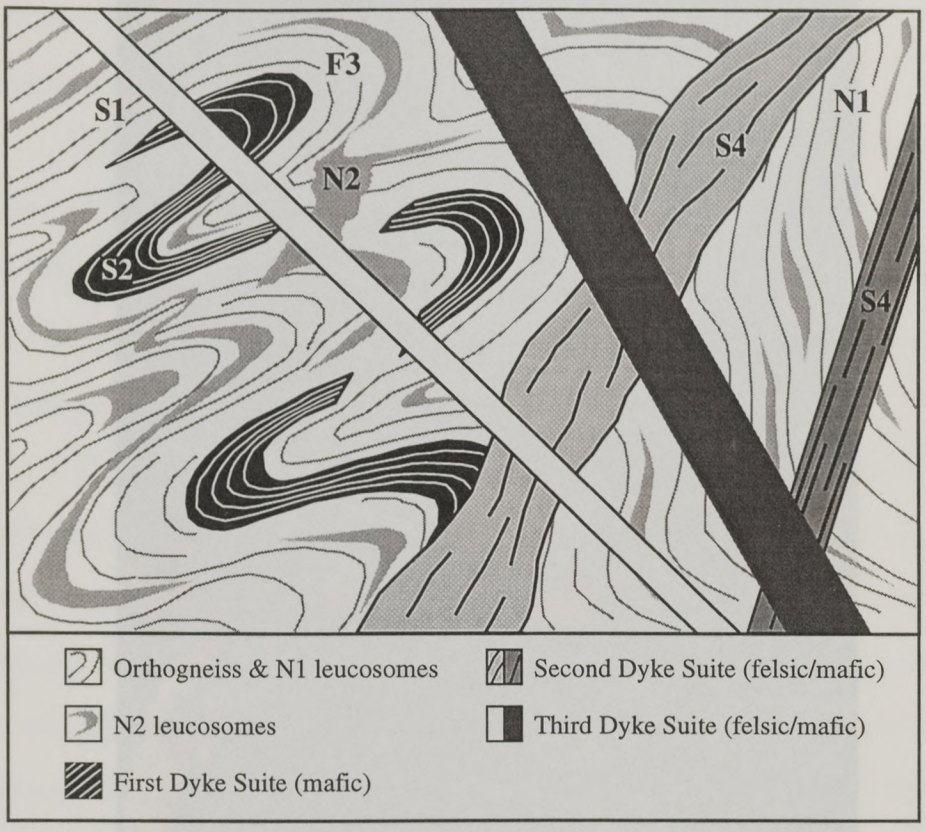

Figure 1.3. Schematic diagram of present-day field relationships, examined to constrain a relative chronology of events in the study area.

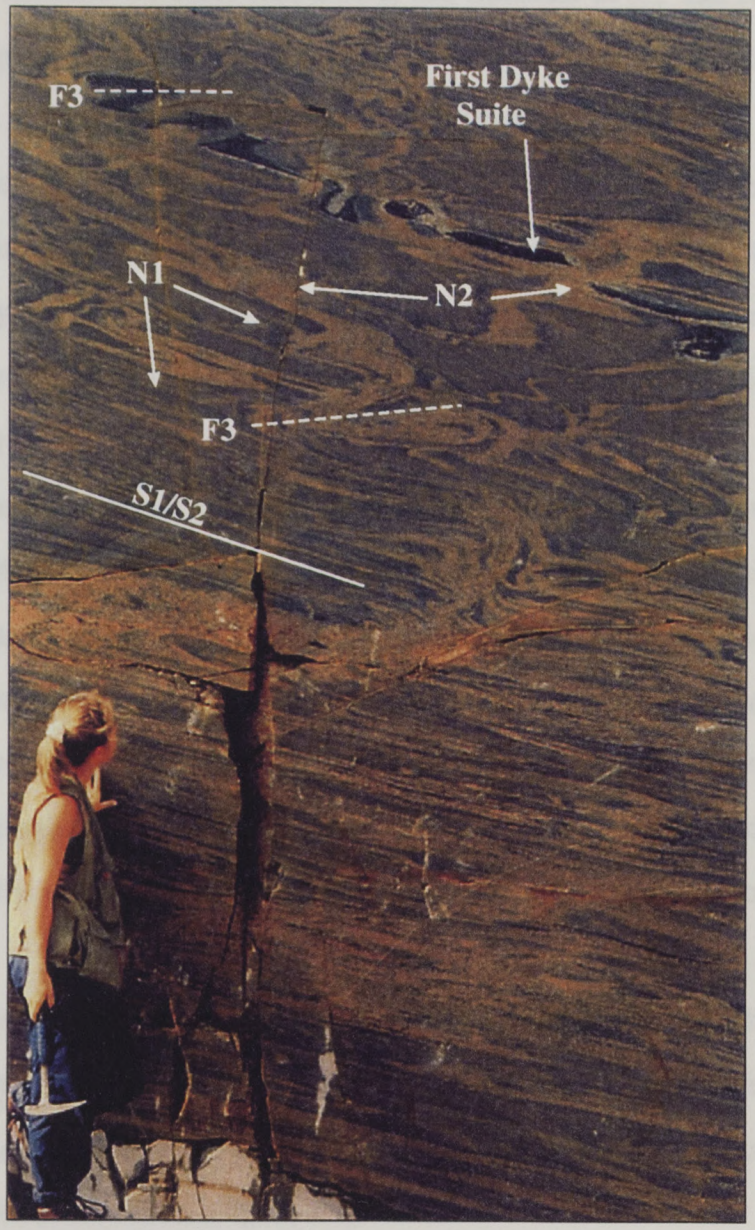

Figure 1.4. D1-D3 structural relationships between S1/S2, N1 and N2 in the felsic orthogneiss. F3 folds fold S1/S2 in the orthogneiss and S2 in the first dyke suite.

Closed to isoclinal F3 folds fold S1/S2, and minerals in N1 and N2 layers are realigned parallel to a weak to moderate S3, axial planar (F3) foliation. A third generation of leucosome (N3) is found locally (Figure 1.5).

The felsic gneiss exhibits a later, well-developed regional lineation (L4). L4 is not ubiquitous, and where present varies from moderate to strong. In N2 and N3 layers it is especially well developed, forming a coarse mineral lineation defined by elongate quartz and feldspar. A corresponding S4 foliation, apparent in younger units, parallels the S1/S2 foliation.

The felsic gneiss contains qtz+pl+kfs±bt±hbl±ms±grt (Appendix A) with biotite and muscovite as either stable or retrograde phases. Muscovite locally displays mimitic growth on biotite. All samples contain accessory zircon, opaque minerals and apatite. Both euhedral and anhedral zircons are present, and many of the crystals contain cores (Figure 1.6). Several samples contain allanite. Twinned plagioclase grains commonly have exsolution lamellae and myrmekitic intergrowths. Chlorite and sericitized plagioclase are products of retrograde reactions.

Most occurrences of the felsic and intermediate gneisses show a highly recrystallized, sugary texture such that distinctive mineral fabrics are rare. Static recrystallization textures, such as straight and cuspate grain boundaries and 120° triple junctions, dominate (Figure 1.7).

Skipås Granite

The Skipås granite, located near Skipås (Figure 1.2) is an approximately 3 km^2, homogeneous, very-fine- to coarse-grained, strongly lineated (L4), felsic

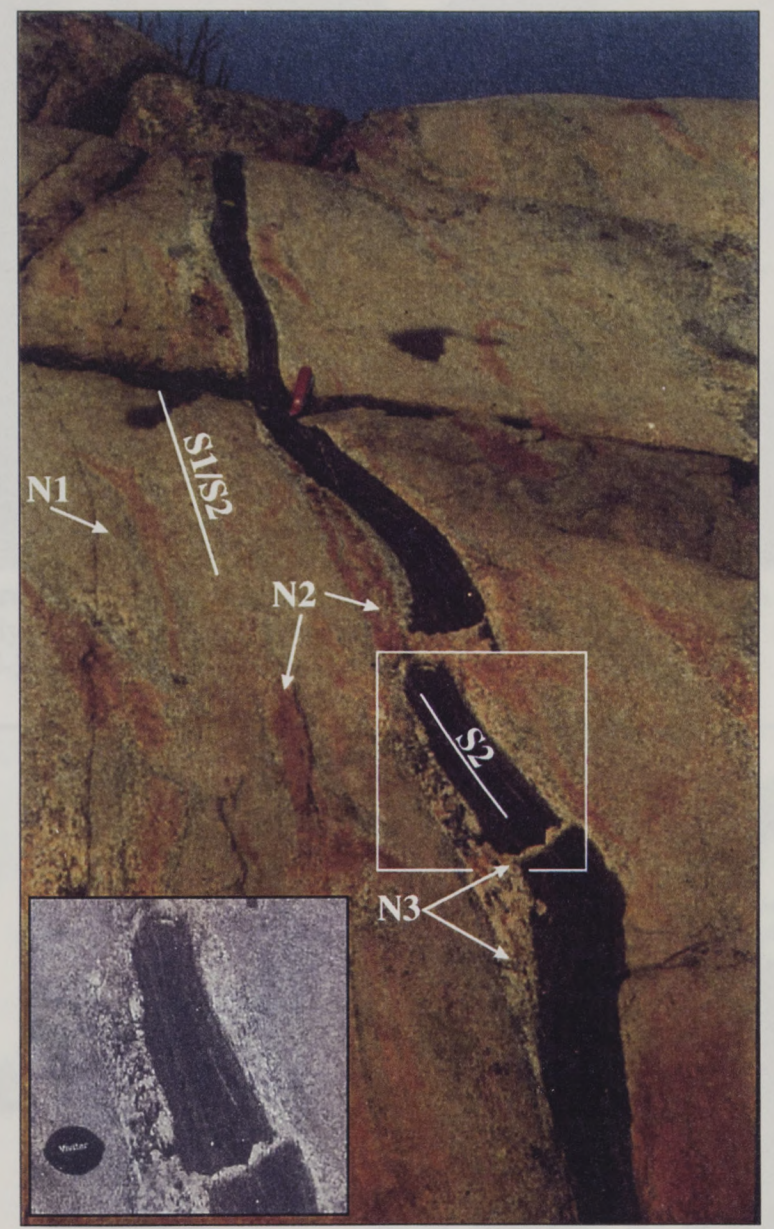

Figure 1.5. Mafic dyke from the first suite intruding the felsic orthogneiss. The dyke shows S2 compositional layering (inset) and boudinage. N2 fills interboudin spaces, and coarser-grained N3 lies along the dyke margin and in interboudin spaces. White box shows area of inset. Pocket knife is 9 cm long.

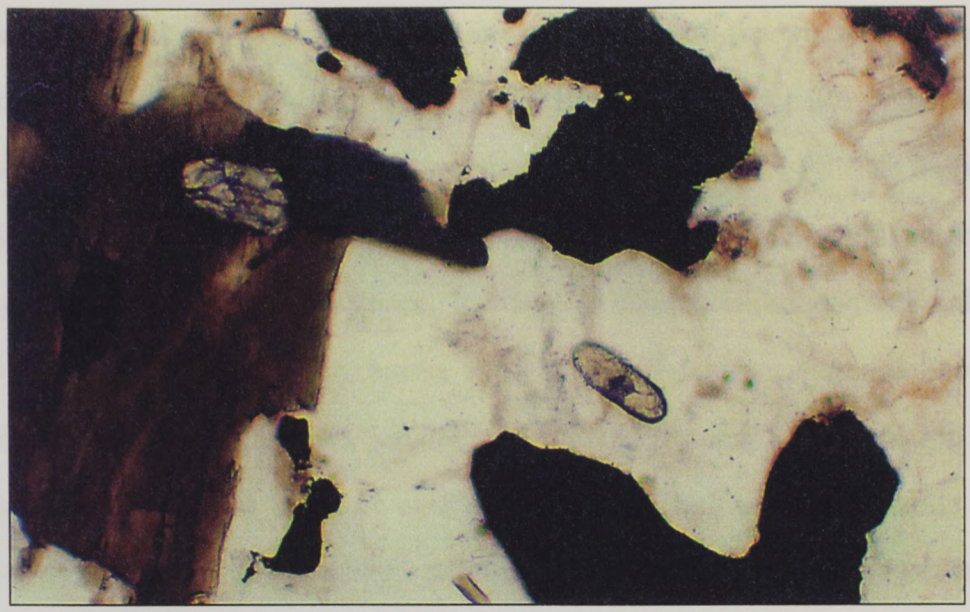

Figure 1.6. Photomicrograph of zircon in a felsic orthogneiss. A core is clearly seen within the zircon. Zircons with cores were carefully avoided for U-Pb geochronology. Field of view is 0.75 mm across.

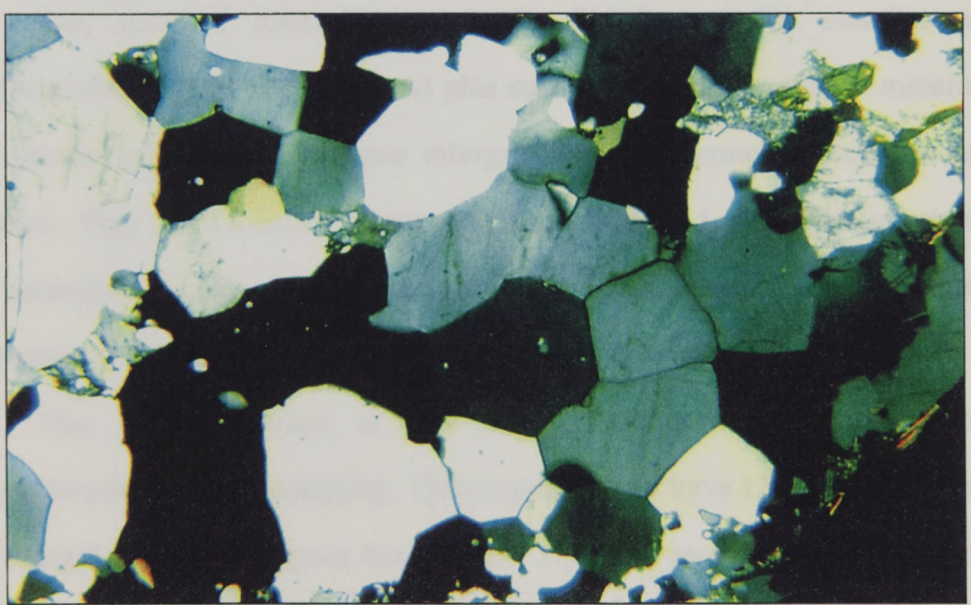

Figure 1.7. Photomicrograph of statically recrystallized quartz and feldspar. This texture is common to all felsic units and indicative of continued metamorphism after Sveconorwegian deformation. Field of view is 3.3 mm across.

orthogneiss that escaped migmatization and much of the gneiss-forming deformation. The strong to very strong L4 lineation of this L-tectonite is defined by aligned elongate K-feldspar augen and quartz ribbons (Figure 1.8). The Skipås granite grades from unfoliated to weakly foliated, with pinch-and-swell contacts between foliated and unfoliated zones. Interlayered quartzo-feldspathic and mafic layers and aligned hornblende, biotite and elongate K-feldspar augen define a weak foliation. The foliation is parallel to the strong, regional S1/S2 foliation in the orthogneisses and is therefore correlated with S1/S2. The Skipås granite is host to dykes that have seen the effects of the regional D2 gneiss-forming event. Field relationships therefore suggest that the Skipås granite is at least as old as the surrounding felsic gneisses, yet its foliation is not nearly as well developed.

The mineral assemblage of the Skipås granite consists of kfs+pl+qtz+hbl±bt±grt (Appendix A) plus subordinate apatite, opaque minerals and zircons with cores. Feldspar intergrowths and myrmekitic textures are common. Very small anhedral garnets and medium-grained poikiloblastic garnets with inclusions of opaques, plagioclase, hornblende and quartz are also common. Retrograde chloritization and sericitization affected the unit.

The Skipås granite is also strongly recrystallized, and static recrystallization textures dominate. Quartz and feldspar have 120° triple junctions and straight and cuspate grain boundaries. Dynamic recrystallization textures indicate rotational recrystallization of quartz and feldspar and migrational recrystallization of quartz by grain boundary migration and bulge nucleation.

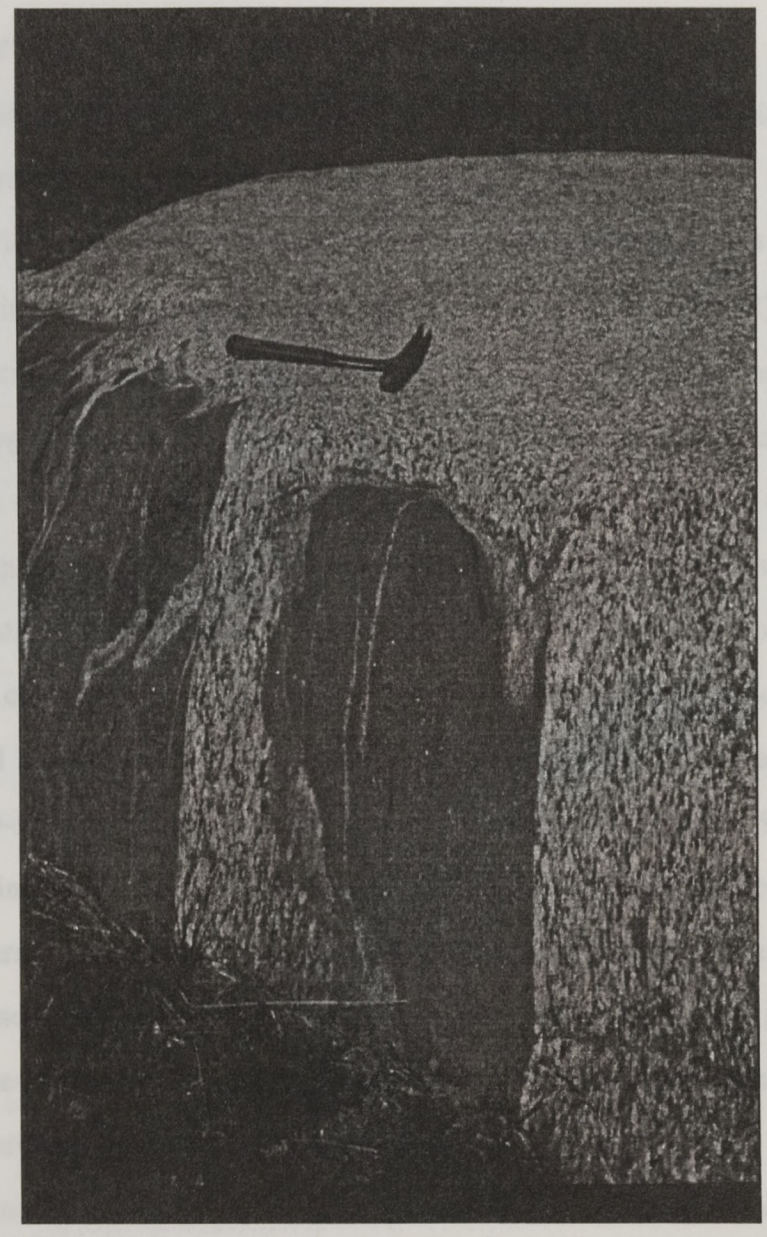

Figure 1.8. Photograph of the Skipås granite. Note the unit's strong linear fabric (L4) and lack of a planar fabric. D2 deformation affected the mafic rocks in the foreground. Rock hammer for scale.

Mafic Amphibolite and Mafic Granulite Orthogneisses

Mafic gneisses are interlayered with the felsic and intermediate gneisses and comprise the second most abundant rock type in the study area. Thicknesses of the mafic gneiss layers range from one meter to approximately 60 meters. All mafic gneisses are S-tectonites with the main gneissic fabric (S1/S2) defined by 0.5 to 10 cm thick compositional layers and less commonly by aligned minerals. Alternating layers of hbl+bt+grt±cpx and plagioclase-rich leucocratic layers define the compositional layering. Aligned hornblende and biotite crystals and elongate quartz ribbons define mineral fabrics. Foliation intensities range from weak to strong planar fabrics, and F3 isoclinally folded S1/S2 compositional layers are common. Some thin (~5 m thick) mafic gneiss layers are boudinaged.

N1 leucosomes vary in appearance from irregularly-shaped aggregates to extremely-flattened and isoclinally folded (F3) stringers (Figure 1.9). Spacing between individual leucosomes varies from tens of centimeters to only a few millimeters. Leucosomes are generally fine grained and contain abundant plagioclase, with lesser abundances of quartz, K-feldspar and garnet. N2 leucosomes occur locally, are coarse grained and are commonly found along the contact between the mafic and felsic gneisses.

Fine- to coarse-grained mafic gneisses have local variations in mineral assemblages, but generally comprise pl+hbl+bt+grt±cpx±qtz±scp±opx±ms (Appendix A). Accessory minerals include anhedral zircon, titanite, opaque minerals and apatite. The mafic gneiss at one locality contains orthopyroxene phenocrysts up to 3 cm in diameter, with retrograde corona textures comprising,

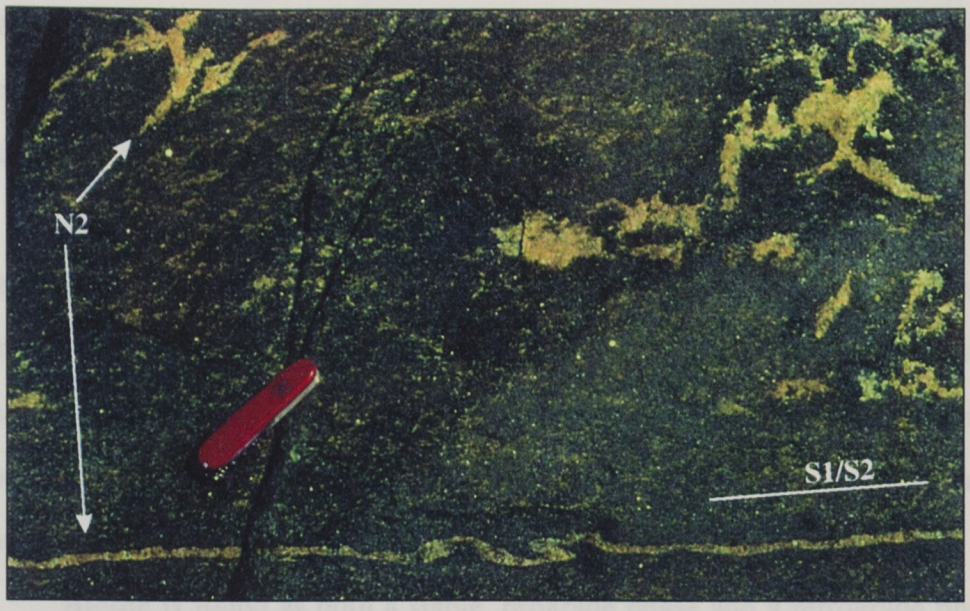

Figure 1.9. Recrystallized mafic orthogneiss, displaying the two end-member styles of leucosomes. The N2 leucosome at the bottom of the photograph is flattened and isoclinally folded, whereas the leucocratic material above and to the right of the pocket knife appears as irregularly shaped aggregates. Pocket knife is 9 cm long.

from core to rim, vermicular intergrowths of clinopyroxene and quartz rimmed by hornblende, quartz, garnet and plagioclase (Figure 1.10). Biotite and opaque minerals are locally present; the opaque minerals display a symplectic texture with clinopyroxene, hornblende and plagioclase (Figure 1.11).

Mineral textures indicate interaction between biotite and hornblende, clinopyroxene and opaque minerals, and clinopyroxene and plagioclase. Garnet with plagioclase coronas and biotite replaced by opaque minerals occur locally. Garnets, up to 7 cm in diameter, occur in several places, locally accompanied by quartz pressure shadows (Figure 1.12). Poikiloblastic garnets with inclusions of hornblende, biotite, plagioclase and zircon are common.

Biotite is found as both a stable, prograde phase and a retrograde phase, and some samples contain multiple generations of biotite. Only samples from Gåsanabbe and Nortorp (Figure 1.2) contain scapolite. Retrograde growth of chlorite and white mica in place of biotite, alteration of hornblende along fractures and grain boundaries to chlorite and chlorite veins are all late-stage textures seen locally. Sericitization of plagioclase is ubiquitous. Moderate to strong static recrystallization textures are pervasive.

Supracrustal Gneisses

One major zone of supracrustal gneiss is found in and around the Stensjö Nature Preserve (Figure 1.2). Differential weathering emphasizes discrete 2 cm to 5 cm thick S1 layers. Leucosomes of very-coarse-grained quartz and feldspar, interlayered with aluminosilicate-bearing paleosome layers, define the dominant S1 foliation. Tight to isoclinal F3 folds asymmetrically fold the foliation (Figure

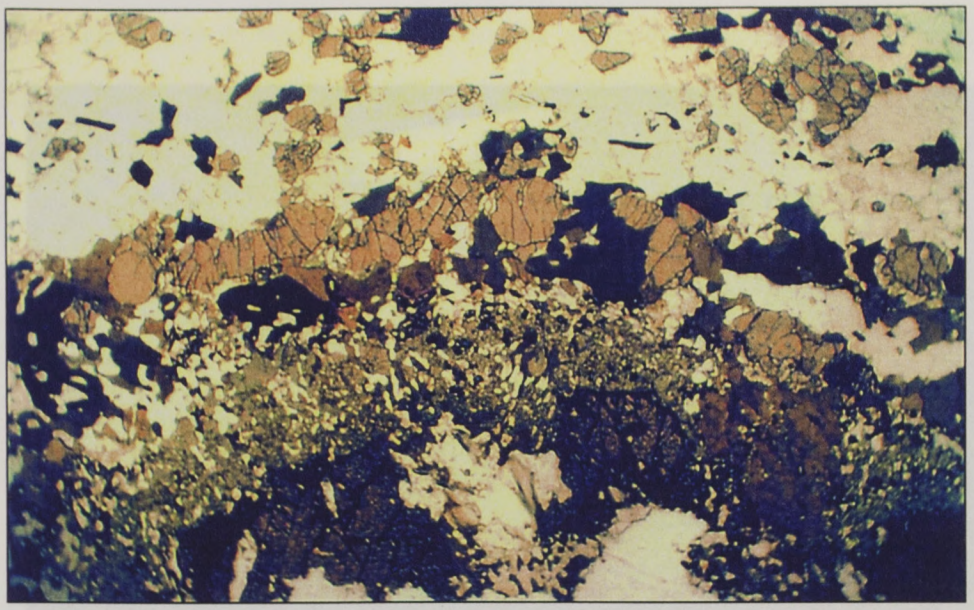

Figure 1.10. Photomicrograph of corona texture in the mafic orthogneiss. Vermicular intergrowths of clinopyroxene and quartz, hornblende, plagioclase and garnet rim orthopyroxene phenocrysts. The field of view is 13 mm across.

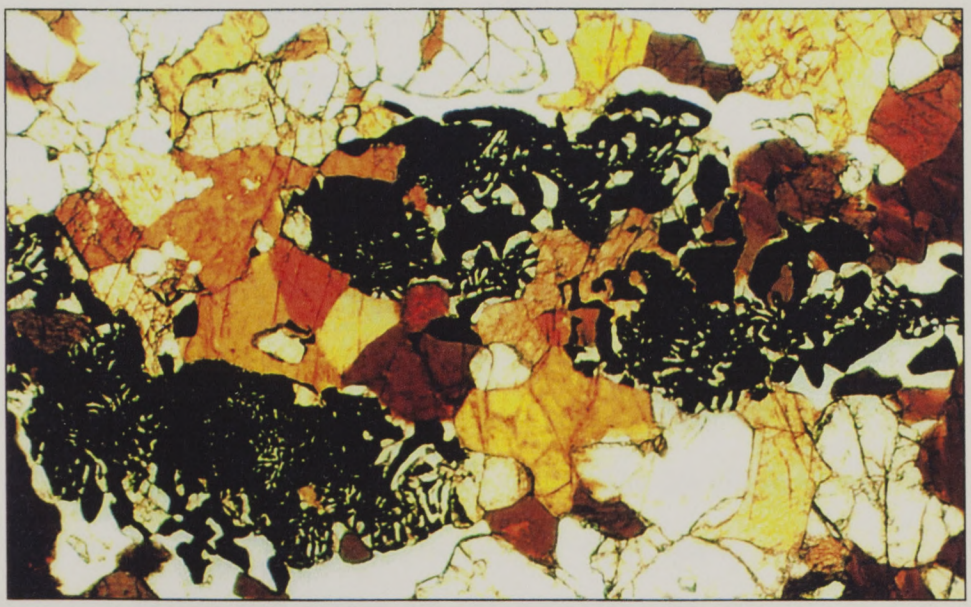

Figure 1.11. Photomicrograph of symplectic texture between opaque minerals, clinopyroxene, hornblende and plagioclase. Field of view is 3.3 mm across.

Figure 1.12. Garnet in a mafic orthogneiss. Note the pressure shadows on either side of the garnet. Pocket knife is 10 cm long.

1.13). Aggregates of weakly to moderately aligned, recrystallized sillimanite needles form a moderate to strong L4 mineral lineation (Figure 1.14) that is commonly oblique to F3 fold axes. Within the Stensjö Nature Preserve, late-stage F5 folding broadly folds the L4 sillimanite mineral lineation (Table 1.1).

The mineral assemblage of the supracrustal gneiss consists of qtz+pl+kfs+sil±bt±ms±hbl±zrn±ap (Appendix A). Biotite occurs in quartz- and feldspar-rich layers and is weakly aligned. Accessory minerals include apatite, titanite, zircon, monazite and tourmaline. Chlorite is a retrograde phase, and plagioclase has been sericitized. The mineral assemblage of the leucosomes is pl+qtz+kfs+grt+bt±ms (Appendix A).

The supracrustal gneisses are strongly recrystallized, as indicated by dynamic and static recrystallization textures in quartz and feldspar and radial sprays of sillimanite. Locally, the supracrustal gneisses are strongly migmatized and resemble orthogneisses; however, the presence of sillimanite maintains the distinction between the supracrustal gneisses and the orthogneisses.

First Dyke Suite (Mafic Dykes)

Mafic dykes of the first suite are polydeformed and thus the oldest observed dykes. These 3 cm to 1 m thick dykes intrude the orthogneisses and are parallel to sub-parallel to the S1 fabric of the gneiss package (Figures 1.3, 1.4, 1.5 & 1.15). Locally, foliations of the host orthogneiss are slightly, but distinctly, oblique to the dyke margins. Millimeter scale mafic layers comprising hornblende, biotite and garnet are interlayered with plagioclase and, less commonly, scapolite layers to define the strong compositional foliation in the

Figure 1.13. Asymmetric F3 folds of S1 in the supracrustal gneiss in the Stensjö Nature Preserve. Sledge hammer for scale.

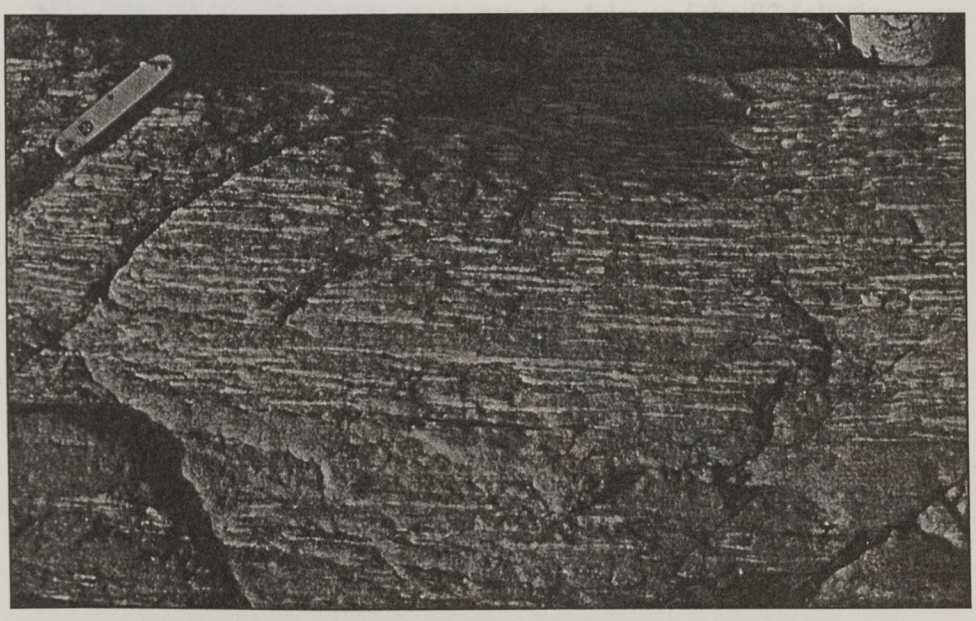

Figure 1.14. Sillimanite lineation (L4) in the supracrustal gneiss in the Stensjö Nature Preserve. Pocket knife is 10 cm long.

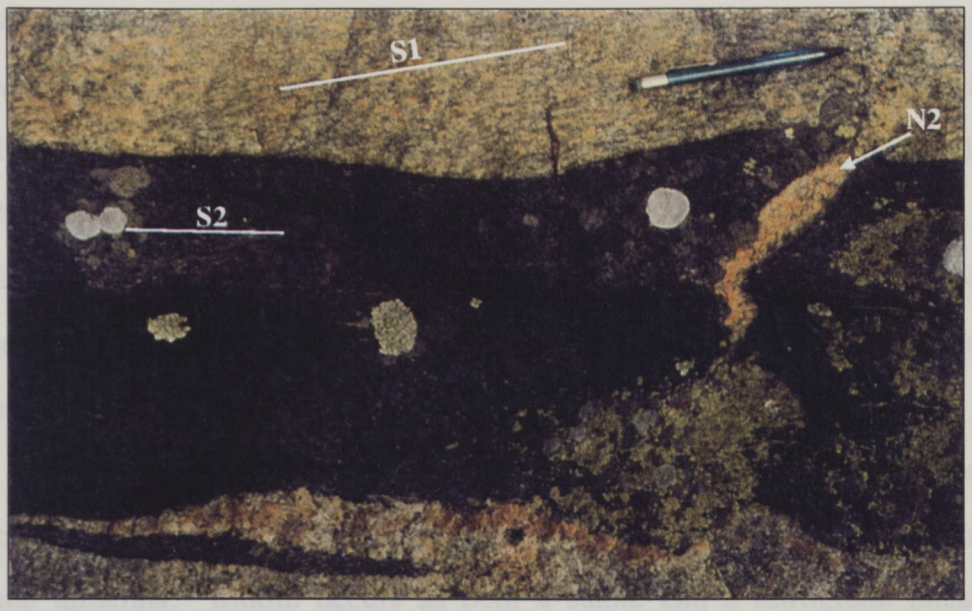

Figure 1.15. Sample 2, a mafic dyke of the first dyke suite. Note the obliquity of S1 in the felsic orthogneiss (parallel to the pencil) to the dyke. N2 of the felsic orthogneiss cross-cuts the dyke and the S2 foliation.

dykes (Figure 1.5). This foliation is correlated with the parallel S2 in the gneisses. Aligned hornblende and biotite complement the compositional layering. At least one generation of leucosome (N2) occurs in the first dyke suite, generally parallel to the S2 foliation. The dykes of the first suite are commonly boudinaged, truncating the S2 foliation. The S2 foliation of the dykes is isoclinally folded (Table 1.1) with a style and orientation similar to F3 folds of N2 in the felsic orthogneiss (Figure 1.4). Folds in the first dyke suite are therefore correlated to F3 in the orthogneisses.

The mineral assemblage of the first dyke suite includes pl+hbl±bt±cpx± grt±qtz±scp (Appendix A). Accessory minerals include zircon, apatite and opaque minerals. Biotite occurs as both a stable and a retrograde phase. Poikiloblastic garnet and hornblende occur locally; garnet includes biotite and clinopyroxene, and hornblende includes plagioclase, opaque minerals and clinopyroxene. Feldspar intergrowth textures are rare. Mineral textures indicate reactions between clinopyroxene and hornblende, and between biotite and hornblende. Chlorite and sericite are retrograde phases with chlorite replacing biotite, and sericite replacing plagioclase. Both dynamic rotational recrystallization and strong static recrystallization features occur in the first dyke suite.

Second Dyke Suite

Both felsic and mafic dykes of the second suite intrude the felsic, mafic and supracrustal gneisses and the first dyke suite. They post-date the earliest deformations, D1, D2 and D3, but predate the D4 deformation (Figure 1.3, Table

1.1). The planar fabrics in the second dyke suite vary widely in intensity and include primary and deformation-related foliations.

Mafic Dykes, Second Dyke Suite

The 15 cm to 2.5 m thick, very-fine-grained to coarse-grained, mafic dykes of the second suite contain a weak planar fabric, S4. Slight compositional variations and, to a lesser extent, aligned hornblende, biotite and elongate, anhedral garnet most commonly define S4. Aligned hornblende also defines a lineation that is correlated with L4 in the gneisses. The lack of migmatitic leucosomes and less deformed nature of these mafic dykes distinguishes them from mafic dykes of the first suite. Mafic dykes of the second suite cross-cut foliations of the migmatitic felsic, mafic and supracrustal gneisses and the first dyke suite, with discordance ranging from slightly oblique to as much as 30°. Field relationships indicate that the second mafic dykes post-date migmatization of the gneisses (Figure 1.16).

The mineral assemblage of these mafic dykes is pl+bt+hbl±cpx±grt±scp± qtz (Appendix A) with accessory opaque minerals, apatite, euhedral zircon, rutile, titanite and calcite. Two generations of biotite exist, but both are rare. Where biotite does occur, it is commonly aligned and mimics earlier foliations. Several reaction rim textures exist including ilmenite rimmed by titanite (Figure 1.17) and, more commonly, clinopyroxene rimmed by hornblende or biotite. Feldspar intergrowths occur in much of the plagioclase. Deformation textures include fractured plagioclase, plagioclase with deformed and displaced twins and kinked plagioclase.

Figure 1.16. Mafic dyke of the second suite (bottom) cross-cutting the mafic orthogneiss. Note the clear evidence that the second dyke suite post-dates the migmatization and gneiss-forming deformation in the orthogneiss. Rock hammer for scale. Photograph was taken at Gåsanabbe.

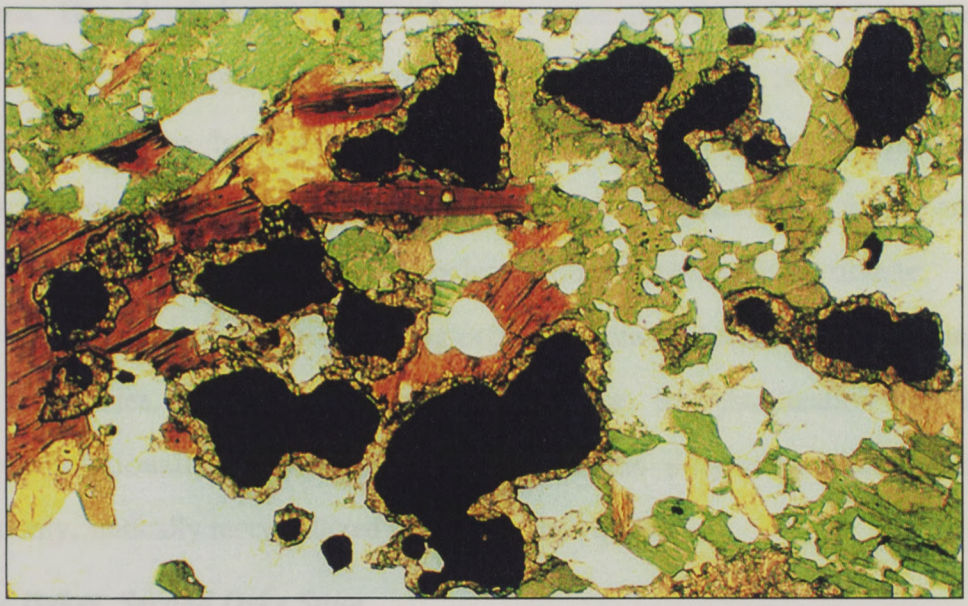

Figure 1.17. Photomicrograph of ilmenite rimmed by titanite in a mafic gneiss. Indicative of retrogression from granulite- to amphibolite-facies conditions. Field of view is 1.7 mm across.

Hornblende, garnet, clinopyroxene and scapolite have poikiloblastic textures. Hornblende has inclusions of opaque minerals, plagioclase, biotite and, less commonly, clinopyroxene. Garnets overgrow the dominant S4 foliation and include plagioclase, hornblende, opaque minerals, biotite and clinopyroxene. Clinopyroxene contains biotite, opaques, plagioclase, hornblende, garnet and rutile needles. Scapolite includes plagioclase, biotite, hornblende and titanite.

Retrograde sericitization of plagioclase commonly occurs near and along grain boundaries. Chlorite is also a retrograde phase. Recrystallization textures include rotationally recrystallized hornblende and plagioclase and, more commonly, statically recrystallized plagioclase and quartz.

Felsic Dykes, Second Dyke Suite

Felsic dykes of the second suite range from aplitic to very coarse grained, with pegmatites as the dominant variety. These dykes range from 10 cm to 2 m thick. Compositional layering of quartz and feldspar defines the main foliation, S4, of these felsic dykes. The foliation, commonly subparallel to the gneissic fabric of the host rock, cross-cuts the S1/S2 foliations of the gneiss units (Figures 1.3, 1.18 & 1.19) and S2 of the first dyke suite. The intensity of deformation varies such that some of the dykes are closed to isoclinally folded by F4 folds and others contain only weak, planar, compositional fabrics. Statically recrystallized quartz and feldspar rods and aligned biotite defined a weak to strong L4 lineation. All dykes are strongly statically recrystallized.

The mineral assemblage consists of kfs+pl+qtz±grt±ms±bt±hbl (Appendix A) with accessory minerals including coarse-grained monazite, well-zoned,

Figure 1.18. Unusually high-angle contact between the mafic orthogneiss (left) and a pegmatite dyke of the second suite (right). Note the weak fabric in the dyke (S4) and the absence of migmatitic leucosomes versus the strong foliation (S1/S2) and presence of leucosomes (N2) in the gneiss. Rock hammer for scale.

Figure 1.19. Structural relationships between the felsic orthogneiss and a pegmatite dyke of the second suite. Sample 3 was extracted from the coarse-grained, dark-pink pegmatite that cross-cuts the flattened N2 leucosomes in the gray, felsic orthogneiss. This photograph shows an apophysis of the sampled dyke. Dashed lines denote margins of the pegmatite. Rock hammer (top) for scale.

euhedral zircons, rounded zircons, rutile and opaque minerals. Garnet phenocrysts reach 1 cm in diameter. Intergrowths between K-feldspar and plagioclase are pervasive. Chlorite and sericite are present as retrograde phases. Static recrystallization is pervasive.

Third Dyke Suite

The third dyke suite represents the last recognizable pulse of intrusive magmatism in the study area. These dyke cross-cut D1-D4 fabrics in all other rock types (Figure 1.3) and contain little evidence of D5 ductile deformation. Compositionally, both pegmatitic and mafic dykes are present, but the former are much more common.

Felsic Dykes, Third Dyke Suite

Pegmatitic dykes of the third suite are widespread and vary in thickness from 1 cm to 3 m. They are coarse to very coarse grained and sometimes yield macroscopic, igneous zircons (<1-5 mm). A representative mineral assemblage is kfs+pl+qtz±bt±zrn (Appendix A). These felsic dykes are commonly undeformed or brittlely tectonized and locally contain kinked biotites. They cross-cut foliations of the other units at high angles, with discordance up to 60°-70°.

Mafic Dykes, Third Dyke Suite

The mafic dykes of the third suite are very fine-grained, indurated rocks, ranging from 3 cm to 3 m wide, that cross-cut fabrics in all felsic and mafic gneiss units as well as in the second dyke suite. Their compositions comprise pl+hbl± cpx±grt±bt±ep±qtz (Appendix A) with accessory opaque minerals, titanite and apatite. Twinned plagioclase laths, a characteristic texture found in igneous

rocks, are preserved. Biotite is weakly aligned. Hornblende and garnet are locally poikiloblastic, with inclusions of plagioclase, biotite and opaque minerals. Chlorite occurs as an alteration product of biotite. Approximately 5 mm wide veins containing plagioclase, hornblende and quartz occur locally. The dykes appear unmetamorphosed in the field, but petrographic studies reveal recrystallization textures including complete static recrystallization of plagioclase and hornblende (Figure 1.20).

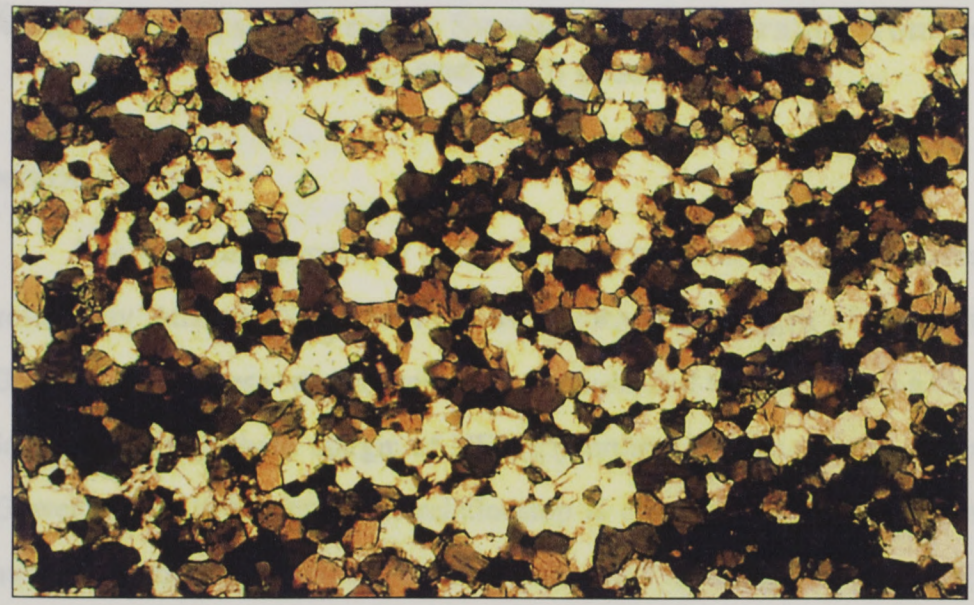

Figure 1.20. Photomicrograph of a statically recrystallized mafic dyke of the third dyke suite. Note the straight grain boundaries and equant grains. Field of view is 3.3 mm across.

Chapter 2: Mesoproterozoic tectonothermal evolution of the Ätran terrane, southwestern Sweden: New constraints from field relationships and U-Pb geochronology

INTRODUCTION

The Grenville Orogen of North America has been correlated across the present-day Atlantic Ocean with the Sveconorwegian Orogen of Scandinavia (Gower, 1990). These two orogenic belts are postulated to have formed a *ca.* 1.70 Ga contiguous southern margin of NENA (Northern Europe - North America) (Gower et al., 1990), but their relationship is complicated because formerly interposed crustal material is now missing. Ongoing studies of the Sveconorwegian Orogen that incorporate field and structural geology with reliable radiometric ages are essential to developing a better understanding of the tectonic evolution of the Baltic craton.

Orogenic events in Baltica include the *ca.* 1.6 Ga Gothian and *ca.* 1.0 Ga Sveconorwegian orogenies (Gower, 1990), and there is limited evidence for an intervening event at *ca.* 1.4 Ga "Hallandian" (Hubbard, 1975). Reworking of pre-existing crustal material during the Sveconorwegian Orogeny produced deformation fabrics that are parallel to earlier-formed fabrics. Assignment of deformation fabrics to their respective orogenic events is a challenge, but fundamental to determining the relative importance of the Gothian and Sveconorwegian orogenies in Baltica.

We have examined a small part of the Southwestern Scandinavian Domain (SSD, Gaál & Gorbatschev, 1987) in southwestern Sweden making outcrop-scale,

structural and petrographic observations and obtaining U-Pb data to help resolve discrepancies in proposed thermotectonic models. A longer-range purpose is to facilitate correlations between thermal and deformational events in southeastern Baltica and eastern Laurentia from Gothian through Sveconorwegian times.

TECTONIC FRAMEWORK OF BALTICA

The Proterozoic tectonic evolution of Baltica was dominated by westward crustal growth (present-day coordinates) away from an Archean core. The 1.95-1.75 Ga Svecofennian Orogeny created a north-south trending belt, the Svecofennian Domain (Figure 1.1) (Gaál and Gorbatschev, 1987). Subsequent eastward subduction under the Baltic craton resulted in 1.85-1.65 Ga calc-alkaline magmatism of the Transscandinavian Igneous Belt (TIB, Lindh & Gorbatschev, 1980; Larson & Berglund, 1992; Persson & Wikström, 1993) forming the western margin of Baltica. Allochthonous arcs were accreted onto this western margin (Åhäll & Gower, 1997) culminating in the 1.75-1.55 Ga collisional event (Connelly et al., 1996), termed the Gothian Orogeny.

The post-Gothian collage of deformed margin (TIB) and accreted arcs is referred to as the Southwest Scandinavian Domain (SSD) (Gaál & Gorbatschev, 1987; Connelly & Åhäll, 1996) and includes the Ätran, Klarälven and Idefjorden terranes (Åhäll & Gower, 1997) (Figure 1.1). The laterally correlated Ätran and Klarälven terranes, formerly known as the Eastern Segment, represent reworked TIB rocks outboard from which lies the allochthounous Idefjorden terrane (Figure 1.1). The Ätran and Klarälven terranes are bound on the east by the Protogine Zone and on the west by the Mylonite Zone, both representing complex ductile

shear zones. Late Gothian, syn-orogenic plutons (1.59-1.55 Ga) stitched arcs of the Idefjorden terrane and this allochthonous terrane to the Ätran terrane (Åhäll et al., 1993; Connelly & Åhäll, 1996).

Gothian orogenesis was followed by widespread inter-orogenic magmatism, sedimentation and rift-related tectonism from *ca.* 1.5 Ga to *ca.* 1.2 Ga (Gorbatschev et al., 1987; Gower et al., 1990; Åhäll & Gower, 1997; Åhäll & Connelly, in press). The episode of inter-orogenic magmatism at *ca.* 1.4 Ga resulted in charnockite bodies and abundant felsic and mafic dykes and may be related to the so-called "Hallandian Orogeny" (Hubbard, 1975). "Hallandian-aged" deformation has been suggested by Hubbard (1976) and Talbot & Heeroma (1989), although, thus far, U-Pb ages from zircons and titanites (Lundqvist et al., 1992; Connelly et al., 1996; Söderlund, 1996) support only a thermal event at this time. Talbot & Heeroma (1989) speculate that deformation near Varberg (Figure 1.2, inset) corresponds to the "Hallandian Orogeny," but deformation associated with this proposed event is not yet understood nor agreed upon.

The SSD was reworked and telescoped during the *ca.* 1.2-0.9 Ga Sveconorwegian Orogeny (Gower, 1990; Hoffman, 1992), the last major event recorded in the SSD. Relatively minor amounts of juvenile crustal material were also added during the Sveconorwegian Orogeny. Early Sveconorwegian contractional deformation was followed by extensional collapse and exhumation of mid-crustal rocks along pre-existing terrane boundaries (Johansson et al., 1991; Connelly et al., 1996; Åhäll & Gower, 1997). Sveconorwegian deformation and metamorphic overprinting were so substantial that some researchers have referred

to the SSD as the Sveconorwegian Province (Gower, 1985; Berthelsen, 1980). We refer to this area as the SSD in recognition of its polydeformed nature.

Parallel to sub-parallel fabrics in the SSD resulting from the Gothian and Sveconorwegian orogenies are nearly indistinguishable without careful examination. Despite this complication, differentiation of Gothian and Sveconorwegian fabrics has been accomplished in some parts of the SSD using cross-cutting relationships between different generations of intrusive rocks (Samuelsson & Åhäll, 1985; Larson et al., 1986; Åhäll et al., 1990; Connelly et al., 1996). Disputes still exist, however, regarding the timing of the migmatization and regional gneiss-formation in the SSD (Åhäll, 1996; Connelly & Åhäll, 1996; Connelly et al., 1996; Johansson et al., 1996; Åhäll et al., 1997b; Möller & Söderlund, 1997). Ages obtained using U-Pb (Söderlund, 1996; Söderlund et al., 1996; Wang et al., 1997), Sm-Nd (Johansson et al., 1991; Johansson & Kullerud, 1993; Wang et al., 1996) and Ar-Ar (Page et al., 1996; Wang et al., 1996, 1997) geochronology, have been interpreted to date a Sveconorwegian gneiss-forming event. In contrast, detailed field mapping and U-Pb geochronology by Connelly & Åhäll (1996), Connelly et al. (1996), Larson (1996) and this study indicate that migmatization and associated deformation occurred primarily during the Gothian Orogeny.

The Ätran Terrane

The Ätran terrane (Figure 1.1) has been mapped at 1:200,000 scale by the Swedish Geological Survey. This terrane comprises mostly 1.70-1.66 Ga, amphibolite- to granulite-facies, felsic and mafic, polydeformed orthogneisses

that are polydeformed equivalents of the TIB rocks (Lindh & Gorbatschev, 1980; Larson et al., 1990; Wahlgren et al., 1994; Connelly et al., 1996; Söderlund et al., 1996). These veined and migmatized orthogneisses have varied compositions including tonalites, granodiorites, quartz-monzonites and granites (Connelly et al., 1996).

Abundant amphibolite- to granulite-facies mafic, granitic and pegmatitic dykes cross-cut the Ätran terrane orthogneisses. Among these, amphibolite-facies dykes yield a wide range of ages, from 1.61 Ga to 1.22 Ga (Berglund & Connelly, 1994; Connelly et al., 1996). A number of structural and geochronologic studies in the Ätran terrane (Welin, 1994; Andersson, 1996; Connelly et al., 1996; Lindh, 1996; Page et al., 1996; Söderlund, 1996; Wang et al., 1996, 1997) have attempted to partition structural and metamorphic elements between the Gothian and Sveconorwegian orogenies. 1612±8 Ma aplitic dykes (Connelly et al., 1996) that cross-cut orthogneisses in the northern Ätran terrane provide the earliest constraint on the timing of Gothian deformation and migmatization in this terrane. Despite the different schools of thought regarding the timing of the major gneiss-forming deformation, it is widely accepted that granulite-facies conditions were locally attained in the Ätran terrane during the Sveconorwegian Orogeny (Johansson et al., 1991; Johansson & Kullerud, 1993; Wang et al., 1997).

The Mylonite Zone

The west-dipping Mylonite Zone (MZ) is a high-grade shear zone that forms the boundary between the upper-amphibolite- to granulite-facies rocks of the Ätran terrane and amphibolite-facies rocks of the Idefjorden terrane (Figure

1.1). Because of the close proximity of this zone to the present study area, it may be locally important. Different studies have suggested a variety of scenarios for the structural history of the kinematically complex MZ (Talbot & Heeroma, 1989; Park et al., 1991; Berglund, 1997). The MZ may be a more ancient zone of weakness, perhaps a Gothian suture between the Ätran and Klarälven terranes and the Idefjorden terrane (Berthelsen, 1980; Gorbatschev, 1980; Park et al., 1991; Åhäll, 1995; Page et al. 1996), or a *ca.* 1.4 Ga "Hallandian" shear zone, as proposed by Talbot & Heeroma (1989).

The break in metamorphic grade across the MZ implies that extension along the zone played a fundamental role in the Sveconorwegian uplift history of the Ätran terrane (Johansson et al., 1991). These authors and Connelly et al. (1996) suggested that the rocks west of the MZ were thrust over the Ätran terrane during the Sveconorwegian Orogeny. Isostatic uplift (Talbot & Heeroma, 1989) and/or gravitational collapse and thermal relaxation of overthickened crust (Larson et al., 1990; Park et al., 1991; Berglund & Connelly, 1994) may explain late Sveconorwegian extension along the MZ.

GEOLOGY OF THE FALKENBERG-HALMSTAD REGION

This study focuses on the coastal region of the Ätran terrane between Falkenberg and Halmstad (Figure 1.2) that comprises amphibolite- and granulite-facies rocks, first identified by Quensel (1951). A number of structural and geochronologic studies (Welin, 1994; Åhäll, 1996; Andersson, 1996; Lindh, 1996; Page et al., 1996; Söderlund, 1996; Wang et al., 1996, 1997) have

attempted to divide structural and metamorphic elements between the Gothian and Sveconorwegian orogenies.

LITHOLOGIES

The study area comprises four major rock units (Table 1.1). Dominant interlayered felsic, intermediate and mafic orthogneisses are the oldest. Two generations of leucosomes, N1 and N2, define the gneissic layering in the orthogneisses (Figures 1.3 & 1.4). A third, coarser-grained, less deformed migmatitic leucosome (N3) is locally present in the felsic orthogneiss (Figure 1.5). N1 and N2 migmatization was accompanied by deformation that transposed primary igneous features. Approximately 3 km^2 of felsic orthogneiss near Skipås (Figure 1.2) escaped migmatization and much of the gneiss-forming deformation, resulting in a more massive, granitic appearance. These rocks are referred to as the Skipås granite.

At least three younger generations of dykes intrude the orthogneisses (Figure 1.3). Dykes of the *first dyke suite* are polydeformed mafic dykes that are parallel to sub-parallel to the earliest fabric (Figures 1.4, 1.5 & 1.15). Coarse-grained leucocratic material that occurs in the first dyke suite is correlated with the N2 phase of the host orthogneiss.

Felsic (chiefly pegmatitic) and mafic dykes of the *second dyke suite* intruded the orthogneisses and cross-cut earlier structural fabrics (Figures 1.3, 1.16, 1.18, 1.19). D4 deformational fabrics dominate in the second dyke suite and vary in intensity.

The *third dyke suite* comprises pegmatitic and mafic dykes and represents the last pulse of magmatism. These dykes intrude all other rock types, cross-cut D1-D4 deformation fabrics and some contain little evidence of D5 deformation (Figure 1.3).

STRUCTURE

Five major phases of ductile deformation (D1-D5) are identified in the study area (Table 1.1). The earliest, D1, affected the orthogneisses and resulted in the first foliation, S1. S1 in the felsic orthogneiss is defined by compositional layers of leucocratic quartzo-feldspathic layers (N1), melanocratic hornblende- and biotite-rich layers and gray, paleosome layers (Figures 1.3 & 1.4). Aligned minerals locally define S1 in the mafic orthogneiss. S1 is cross-cut by N2 and all three dyke suites (Figures 1.15, 1.16, 1.18 & 1.19).

The second phase of deformation, D2, enhanced the foliation in the orthogneisses and flattened N2 creating a composite S1/S2 foliation (Figure 1.4; Table 1.1). D2 also produced an S2 compositional layering in the first dyke suite, defined by hornblende-biotite-garnet layers and plagioclase-rich leucocratic layers (N2) (Figure 1.5). Aligned hornblende and biotite compliment the S2 compositional layering. In addition to producing a foliation, late-stage D2 deformation resulted in boudinage of the first dyke suite with N2 leucosomes of the felsic orthogneiss filling the interboudin spaces. Thus, both N2 leucosomes formed and were flattened during D2. The second and third dyke suites cross-cut S2.

Closed to isoclinal folds (F3) of both S1/S2 of the gneisses and S2 of the first dyke suite characterize the third phase of deformation, D3 (Figures 1.4 & 1.13; Table 1.1). Realigned quartz and feldspar augen locally define a weak F3 axial planar foliation (S3). The slight discordance of S3 with earlier foliations makes it difficult to differentiate between S1/S2 and S3 in the field in the absence of F3 folds. Thus, on the limbs of F3 folds, D3 resulted in a composite S1/S2/S3 foliation. The second and third dyke suites are not observed to cross-cut D3 structures.

The fourth phase of deformation, D4, affected the gneisses and the first and second dyke suites and produced structures that are parallel to subparallel to those of D1-D3. D4 structures include an S4 foliation that is axial planar to F4 open to isoclinal folds, and a regional L4 lineation, as noted by Åhäll (1996) (Table 1.1). F4 folds refold F3 folds. S4, most easily seen in the second dyke suite, is commonly defined by compositional layers and locally defined by mineral alignment. S4 is typically subparallel to but unequivocally cross-cutting the composite foliation of the host gneiss (Figures 1.16 & 1.18). L4, typically south to southeast plunging, is most commonly a mineral elongation or alignment. Felsic, pegmatitic dykes of the second suite and felsic and intermediate gneisses display a strong to weak L4. The third dyke suite cross-cuts D4 structures.

The last phase of deformation, D5, affected the gneisses, the first and second dyke suites and some dykes of the third suite (Table 1.1). D5-related shear zones locally cross-cut the gneisses and the second dyke suite. D5 reoriented D1-D4 fabrics by broad, open F5 folds with north trending fold axes. D5 structures are not ubiquitous in the dykes of the third suite, however some are

folded (F5). Later, brittle deformation affected some dykes of the third suite, but many of these dykes are undeformed.

METAMORPHISM

Little can be determined about the nature of pre-Sveconorwegian metamorphism because mineral assemblages and recrystallization textures in rocks throughout southwestern Sweden formed during the Sveconorwegian Orogeny (Johansson et al., 1991; Johansson & Kullerud, 1993; Wang et al., 1997). Field relationships between N1 and N2 leucosomes and the cross-cutting dykes of the second dyke suite, and geochronologic evidence discussed below, however, support Gothian-aged migmatization, indicating that temperatures were high enough to induce partial melting at that time. The association of N1 and N2 with the D1 and D2 deformation phases, respectively, suggest that Gothian migmatization was attendant with D1 and D2 deformations.

F3 fold style weakly constrains the metamorphic conditions during D3. Both mafic dykes of the first suite and N2 in the felsic orthogneiss form passive F3 folds, indicating similar rheological behavior. Such similar rheological properties in rocks with such varied compositions suggests that D3 deformation occurred at high temperatures.

Maximum Sveconorwegian-aged P-T conditions estimated by Johansson et al. (1991) for the southernmost part of the present study area are 10.5 kbar and 705°C. Isotopic studies by Johansson et al. (1991), Page et al. (1996), Söderlund (1996) and Wang et al. (1997) in this area provide a wide range of ages from *ca.* 1.0 Ga to *ca.* 0.9 Ga. We have been able to substantiate reported granulite-facies

assemblages in the area (Söderlund, 1993, 1996; Johansson et al., 1996) in only one locality; otherwise the assemblages are amphibolite- to upper-amphibolite-facies.

In the one exceptional occurrence, 3 cm orthopyroxene porphyroblasts with corona textures suggest granulite-facies conditions with retrogression to amphibolite- or upper-amphibolite-facies. The 1 cm coronas include, from core outward, vermicular intergrowths of clinopyroxene and quartz, rimmed by hornblende, quartz, garnet and plagioclase (Figure 1.10). Opaque minerals locally display a symplectic texture comprising clinopyroxene, hornblende and plagioclase (Figure 1.11). Possible reactions that would produce these disequilibrium textures include pl+opx --> grt+qtz or pl+hbl --> grt+qtz+H_2O.

Other mineral textures in mafic rocks suggest retrograde reactions such as 1) hbl+qtz --> bt+pl, 2) grt+qtz --> pl+H_2O and Ca-rich fluid and 3) cpx+Ca-rich pl+H_2O --> hbl+Na-rich pl. Ilmenite rimmed by titanite indicates a local breakdown reaction of ilmenite to titanite (Figure 1.17). Ilmenite is common in granulite-facies orthogneisses (Deer et al., 1992), thus its breakdown is consistent with granulite-facies conditions and subsequent retrogression.

Recrystallization textures indicate minimum peak metamorphic conditions. Dynamic recrystallization textures seen in many felsic rocks include migrationally recrystallized quartz, minor amounts of migrationally recrystallized feldspar, and rotationally recrystallized quartz and feldspar. Such textures are common to upper-amphibolite- to granulite-facies rocks. Pervasive static recrystallization of quartz and feldspars (Figures 1.7 & 1.20) implies that metamorphism continued after Sveconorwegian deformation ceased.

GEOCHRONOLOGY

Having established the relative timing of events using field relationships, U-Pb geochronology was employed to gain a better understanding of the tectonothermal development of the region. Geochronology samples were selected to determine and/or constrain ages of magmatism, migmatization and metamorphism. Specific objectives were: 1) determine the crystallization age of the protolith of the felsic gneiss unit, 2) determine the age of metamorphism of the mafic gneisses, 3) constrain the timing of emplacement and metamorphism of the first dyke suite, 4) verify the *ca.* 1.4 Ga crystallization age of the second dyke suite as previously determined by Söderlund (1996), 5) resolve the timing of the regional gneiss-forming event, 6) constrain the timing of Sveconorwegian deformation as related to the crystallization of an undeformed dyke from the third dyke suite and 7) estimate the rate of late- to post-Sveconorwegian cooling. Appendix B outlines U-Pb analytical procedures; sample locations follow the sample numbers below and are given using coordinates of the Swedish National Grid.

Analytical Results

Paleosome, Sample 1 (629740/130691)

Sample 1, a gray, homogeneous layer in the felsic gneiss, representing its paleosome, was collected from an abandoned coastal quarry near Särdal (Figure 1.2). Abundant leucosomes and veins were carefully avoided during sampling. Zircon morphologies range from euhedral, prismatic and elongate grains to anhedral ellipses and spheres. Cores, apparent using petrographic and

cathodoluminescence (CL: Appendix C) microscopy, are common in the euhedral grains, and care was taken to avoid grains containing them. Titanite occurs as light orange to medium brown fragments.

U-Pb isotopic data (Table 2.2) from five clear, colorless fractions (Z1, Z3, Z4, Z5, Z6) of euhedral igneous zircons (Figure 2.21, CL inset), 2 μg (single grain) to 40 μg, define a discordia line with an upper intercept (U.i.) of 1659±5 Ma and a lower intercept (L.i.) of 872+71/-66 Ma (probability of fit 12%; Figure 2.21). In spite of the statistically acceptable regression of this line, data from zircon fractions Z5 and Z6 plot concordantly at 1664±4 Ma, a value located within the estimated error for the U.i. Therefore, 1664±7 Ma is preferred and is interpreted to represent the crystallization age of the igneous protolith.

Two titanite fractions yield a concordant age of 932±7 Ma (Figure 2.21, inset) that reflects local metamorphism. Estimated closure temperatures for the U-Pb system in titanite range widely from 450°C to >700°C (Mattinson, 1978; Gascoyne, 1986; Tucker et al., 1987; Heaman & Parrish, 1991; Mezger et al., 1991; Mezger et al., 1993; Scott & St-Onge, 1995; Zhang & Schärer, 1996). Concordant data from the two titanite fractions agree within error with the L.i. for the zircon regression at 932±7 Ma, interpreted as the age of metamorphism that resulted in Pb loss in zircon.

Data from zircon fractions Z2 and Z7 (Figure 2.21) plot above the discordia line. These fractions possibly experienced multi-stage Pb loss and/or overgrowth during one or more metamorphic events preceding *ca.* 932 Ma.

Table 2.2. U-Pb isotopic data.

Fraction	Weight [mg]	Concentration U [ppm]	Concentration Pb rad [ppm]	Measured total common Pb [pg]	Measured $^{206}Pb/^{204}Pb$	Corrected Atomic Ratios* $^{208}Pb/^{206}Pb$	Corrected Atomic Ratios* $^{206}Pb/^{238}U$	Corrected Atomic Ratios* $^{207}Pb/^{235}U$	Corrected Atomic Ratios* $^{207}Pb/^{206}Pb$	Ages [Ma] $^{206}Pb/^{238}U$	Ages [Ma] $^{207}Pb/^{235}U$	Ages [Ma] $^{207}Pb/^{206}Pb$
Paleosome (sample 1)												
Z1 med clr rnd abr	0.033	226	66.1	124	1064	0.1222	0.27785 98	3.8357 152	0.10012 12	1581	1600	1626
Z2 med clr el need abr	0.043	195	57.5	213	716	0.1244	0.28076 112	3.8640 168	0.09982 24	1595	1606	1621
Z3 med clr el abr	0.033	192	56.9	6	17796	0.1283	0.27954 430	3.8627 590	0.10022 18	1589	1606	1628
Z4 med clr prsm abr	0.040	111	32.7	12	6274	0.1264	0.27972 86	3.8565 118	0.09999 12	1590	1605	1624
Z5 1 lg clr prsm abr	0.006	162	51.6	3	6094	0.1563	0.29450 100	4.1488 132	0.10217 18	1664	1664	1664
Z6 1 lg clr prsm abr	0.004	123	39.7	3	3828	0.1737	0.29543 262	4.1526 366	0.10194 20	1669	1665	1660
Z7 1 med clr el euh abr	0.002	230	67.0	6	1595	0.1221	0.27747 124	3.7561 188	0.09818 32	1579	1583	1590
T1 med clr brn frag abr	0.081	112	28.4	156	588	0.8156	0.15570 58	1.5091 78	0.07029 24	933	934	937
T2 med clr ylw abr	0.104	113	27.0	189	622	0.7120	0.15501 56	1.5005 64	0.07020 16	929	931	934
Mafic dyke, first dyke suite (sample 2)												
Z1 16 best sm clr abr	0.012	305	91.7	4	14350	0.1565	0.27782 102	3.8185 144	0.09968 14	1580	1597	1618
Z2 sm clr incl rnd abr	0.010	673	167.5	8	13291	0.1129	0.23973 84	3.0963 104	0.09367 14	1385	1432	1502
Z3 sm clr rnd ir abr	0.013	409	112.5	7	11545	0.1425	0.25766 128	3.4474 138	0.09704 30	1478	1515	1568
Z4 sm clr-frac rnd abr	0.017	566	149.8	8	18454	0.1354	0.24998 114	3.2828 132	0.09524 24	1438	1477	1533
Z5 sm lt yw ir eq abr	0.015	512	160.6	32	4326	0.2188	0.27608 96	3.8410 144	0.10091 12	1572	1601	1641
Pegmatite dyke, second dyke suite (sample 3)												
Z1 lg clr euh prsm abr	0.027	260	69.4	5	22541	0.1859	0.24326 78	3.0091 102	0.08972 10	1404	1410	1419
Z2 lg clr euh frag abr	0.047	256	68.9	6	32692	0.1798	0.24607 86	3.0510 112	0.08992 10	1418	1420	1424
Z3 lg clr euh frag abr	0.041	231	60.8	3	42962	0.1692	0.24252 72	2.9972 98	0.08963 10	1400	1407	1418
Z6 lg clr-frac euh abr	0.101	240	63.1	8	46575	0.1691	0.24239 82	2.9999 110	0.08976 8	1399	1408	1420
M2 3 med clr lt yw rnd	0.028	339	2440.8	26	4281	43.1061	0.18762 54	2.0437 58	0.07900 10	1108	1130	1172
M3 1 v lg clr yw blocky	0.014	206	2805.8	23	2031	63.6125	0.24310 76	2.9841 88	0.08903 14	1403	1404	1405
M4 1 v lg clr yw blocky	0.022	1065	2589.3	16	14071	16.5857	0.15884 52	1.5499 52	0.07077 6	950	950	951
M5 1 v lg clr yw blocky	0.008	578	1846.6	8	6228	22.1250	0.15895 68	1.5523 58	0.07083 16	951	951	953
M6 1 v lg clr yw blocky	0.013	524	2095.9	10	6564	28.0825	0.15819 40	1.5406 38	0.07063 10	947	947	947
R1 lg clr gold el abr	0.200	5	0.6	41	229	0.0309	0.14602 246	1.3758 242	0.06833 58	879	879	879
R2 med clr gold el abr	0.205	4	0.6	62	146	0.0444	0.14944 78	1.4421 144	0.06999 60	898	907	928
Pegmatite dyke, second dyke suite (sample 4)												
Z1 lg clr rnd eq abr	0.056	897	192.3	153	4548	0.0464	0.22033 54	2.5883 66	0.08520 6	1284	1297	1320
Z2 lg rnd frac	0.012	1152	267.9	26	7995	0.0456	0.23866 56	2.9007 72	0.08815 6	1380	1382	1386
Z3 1 clr rnd abr	0.003	1134	262.4	7	7387	0.0424	0.23796 82	2.8962 94	0.08827 16	1376	1381	1388

Mafic gneiss (sample 5)														
Z1 sm clr eq rnd abr	0.031	327	78.4	125	1256	0.0693	0.24049	72	2.9608	100	0.08929	14	1389	1398	1410
Z2 v sm clr eq rnd abr	0.007	372	87.4	5	7773	0.0444	0.24114	104	2.9757	122	0.08950	20	1393	1401	1415
Z4 sm clr rnd eq abr	0.014	97	22.0	13	1570	0.0570	0.23094	102	2.8090	110	0.08822	24	1339	1358	1387
Z5 v sm clr rnd eq abr	0.012	212	49.1	7	5576	0.0488	0.23691	86	2.9096	94	0.08907	18	1371	1384	1406
T1 lg clr dk brn frag	0.131	275	42.9	136	2595	0.0960	0.15540	60	1.5042	62	0.07021	10	931	932	934
T2 lg clr lt yw frag	0.112	43	7.0	131	372	0.1540	0.15594	82	1.5099	100	0.07023	38	934	934	935
Pegmatite dyke, third dyke suite (sample 6)															
Z1 1 v lg pk frag abr	0.181	208	32.1	93	3920	0.0946	0.15413	46	1.5024	50	0.07069	10	924	931	949
Z3 1 best clr frag abr	0.010	258	39.9	7	3947	0.0738	0.15751	68	1.5345	64	0.07066	18	943	944	947
Z4 1 clr frag abr	0.025	293	44.6	4	16214	0.0625	0.15628	56	1.5206	60	0.07057	20	936	939	945
Skipås granite (sample 7)															
Z1 med clr rnd abr	0.019	362	106.5	114	1099	0.1204	0.27978	126	3.8988	194	0.10107	34	1590	1613	1644
Z2 sm el incl frac abr	0.022	349	94.9	17	7354	0.0952	0.26474	92	3.5685	130	0.09776	14	1514	1543	1582
Z3 med clr incl abr	0.013	439	120.2	19	5165	0.0949	0.26666	80	3.6390	120	0.09898	10	1524	1558	1605
Z4 lg incl clr euh el	0.005	324	96.5	5	5085	0.1287	0.28096	102	3.9406	126	0.10172	22	1596	1622	1656

Codes in fraction numbers are: M, monazite; R, rutile; T, titanite; Z, zircon.

Abbreviations are: abr, abraded; brn, brown; clr, clear; dk, dark; el, elongate; eq, equant; euh, euhedral; frac, fractures; frag, fragments; incl, inclusions; ir, irregular; lt, light; lg, large; med, medium; need, needles; pk, pink; prsm, prism; rnd, round; sm, small; v, very; yw, yellow.

*Ratios corrected for fractionation, 2-3 pg laboratory Pb blank, initial common Pb calculated using Pb isotopic compositions of Stacey and Kramers (1975) and 1 pg U laboratory blank. Two-sigma uncertainties on isotopic ratios, calculated with a modified unpublished error propagation program written by L. Heaman, are reported after the ratios and refer to the final digits.

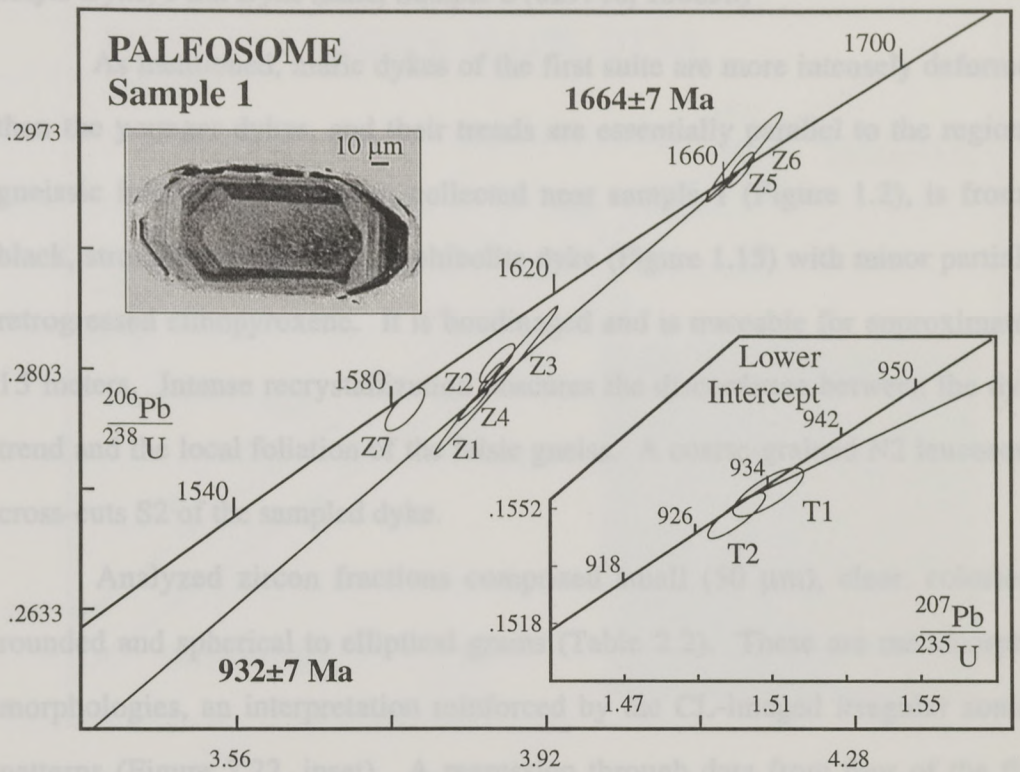

Figure 2.21. Concordia diagram for sample 1, zircon (Z) and titanite (T; inset). Below the sample label is a CL image of an igneous zircon from sample 1 showing euhedral growth zoning. See text for discussion.

Mafic Dyke, First Dyke Suite, Sample 2 (629748, 130693)

As mentioned, mafic dykes of the first suite are more intensely deformed than the younger dykes, and their trends are essentially parallel to the regional gneissic foliation. Sample 2, collected near sample 1 (Figure 1.2), is from a black, strongly foliated (S2) amphibolite dyke (Figure 1.15) with minor partially retrogressed clinopyroxene. It is boudinaged and is traceable for approximately 15 meters. Intense recrystallization obscures the discordance between the dyke trend and the local foliation of the felsic gneiss. A coarse-grained N2 leucosome cross-cuts S2 of the sampled dyke.

Analyzed zircon fractions comprised small (50 μm), clear, colorless, rounded and spherical to elliptical grains (Table 2.2). These are metamorphic morphologies, an interpretation reinforced by the CL-imaged irregular zoning patterns (Figure 2.22, inset). A regression through data from four of the five fractions yields an U.i. of 1654±9 Ma (probability of fit 10%; Figure 2.22), interpreted as a metamorphic age. The L.i., 941±30 Ma, is interpreted as a product of Sveconorwegian Pb loss. Excluded from the regression is the datum for fraction Z5, that lies below the discordia line and is interpreted to indicate an inherited component.

Pegmatite Dyke, Second Dyke Suite, Sample 3 (629729/130691)

Sample 3 is a coarse-grained and strongly lineated (L4) pegmatite collected from an approximately 30 m^3 outcrop near the sample 1 and 2 localities (Figure 1.2). The pegmatite cross-cuts the fabric (S1/S2) of the host felsic gneiss

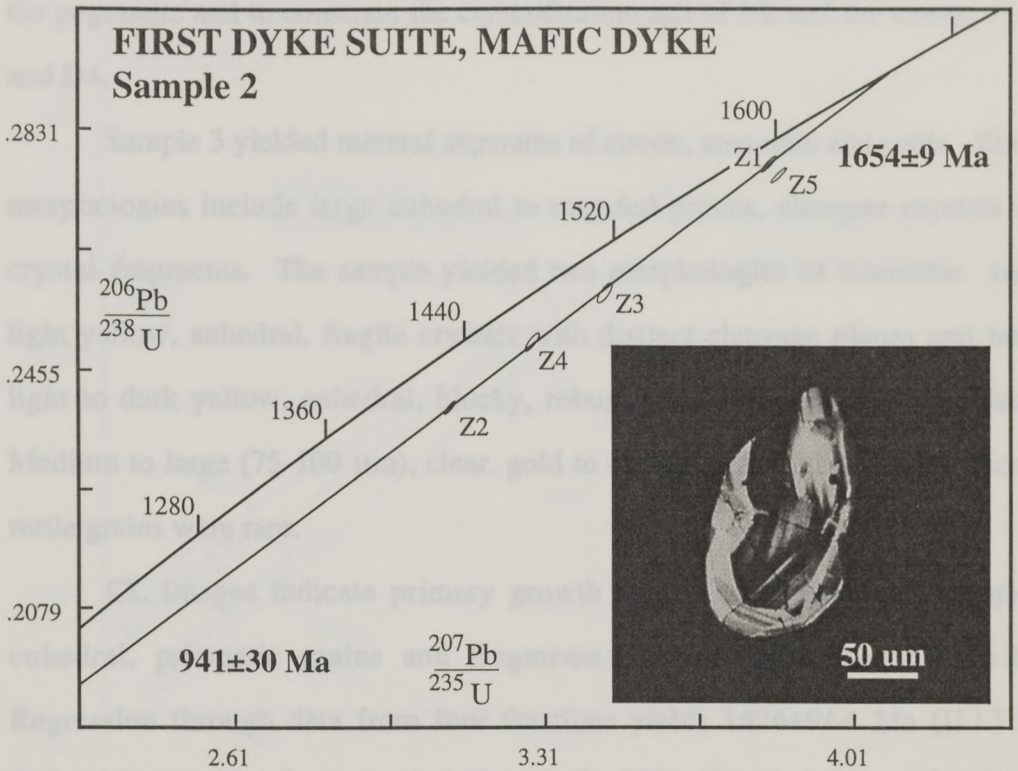

Figure 2.22. Concordia diagram for sample 2, zircon (Z). Inset is a CL image of a metamorphic zircon from sample 2. See text for discussion.

(Figure 1.19), and was collected to determine the igneous crystallization age of the pegmatite and to constrain the crystallization age of N2 and the timing of D2 and D4.

Sample 3 yielded mineral separates of zircon, monazite and rutile. Zircon morphologies include large euhedral to rounded prisms, elongate crystals and crystal fragments. The sample yielded two morphologies of monazite: large, light yellow, anhedral, fragile crystals with distinct cleavage planes and large, light to dark yellow, anhedral, blocky, robust grains lacking cleavage planes. Medium to large (75-100 μm), clear, gold to orange, euhedral and multi-faceted rutile grains were rare.

CL images indicate primary growth zoning in large, clear, colorless, euhedral, prismatic grains and fragments of analyzed zircon (Table 2.2). Regression through data from four fractions yields 1426+9/-4 Ma (U.i.) and 517+307/-227 Ma (L.i.) (probability of fit 26%; Figure 2.23). The U.i. is interpreted to represent the igneous crystallization age of the pegmatite. In the context of the known geologic history of the region, the L.i. is possibly a consequence of progressive and/or multi-stage Pb loss.

Copeland et al. (1988), Parrish (1990) and Mezger et al. (1991) maintain that monazite forms during moderately high-grade metamorphism (T = 640°-750°C), and that monazite U-Pb ages refer to cooling through amphibolite facies (Copeland et al., 1988). Data from five monazite fractions produce a mixing line between 1410±9 Ma (U.i.) and 948±4 Ma (L.i.) (probability of fit 60%; Figure 2.23, inset). Fractions M3-M6 are single-grain analyses that indicate two separate events. The first, dated by the fragile crystal morphology at 1410±9 Ma, most

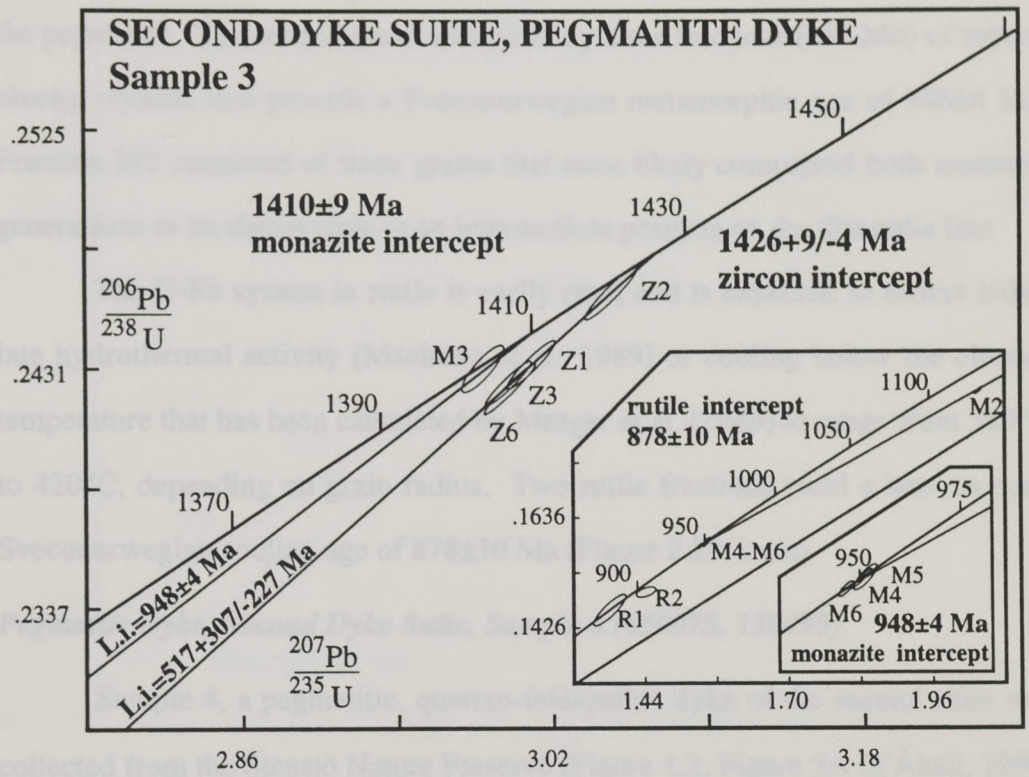

Figure 2.23. Concordia diagram for sample 3, zircon (Z), monazite (M; inset) and rutile (R; inset). See text for discussion.

likely represents the age of monazite crystallization during the initial cooling of the pegmatite. The second event was dated by three fractions (M4-M6) of robust, blocky crystals that provide a Sveconorwegian metamorphic age of 948±4 Ma. Fraction M2 consisted of three grains that most likely comprised both monazite generations as its datum plots in an intermediate position on the discordia line.

The U-Pb system in rutile is easily reset and is expected to reflect either late hydrothermal activity (Machado et al., 1989) or cooling below the closure temperature that has been calculated by Mezger et al. (1989) to range from 380°C to 420°C, depending on grain radius. Two rutile fractions yield a late- to post-Sveconorwegian cooling age of 878±10 Ma (Figure 2.23, inset).

Pegmatite Dyke, Second Dyke Suite, Sample 4 (630075, 130495)

Sample 4, a pegmatitic, quartzo-feldspathic dyke of the second suite was collected from the Stensjö Nature Preserve (Figure 1.2, Figure 2A in Åhäll, 1996, p. 191). The pegmatite cross-cuts S1/S2 of the host felsic gneiss and has a weak compositional foliation (S4). Determination of a crystallization age constrains the timing of D1 and D2 deformations affecting the host gneiss and the timing of S4 formation in the dyke.

Zircon morphologies include large, rounded, clear, colorless, equant grains that are commonly cracked. Data from U-Pb analyses of three zircon fractions yield a discordia line with an U.i. of 1399+7/-6 Ma and a L.i. of 988+33/-32 Ma (probability of fit 12%; Figure 2.24). The U.i. age is interpreted to refer to crystallization of the dyke.

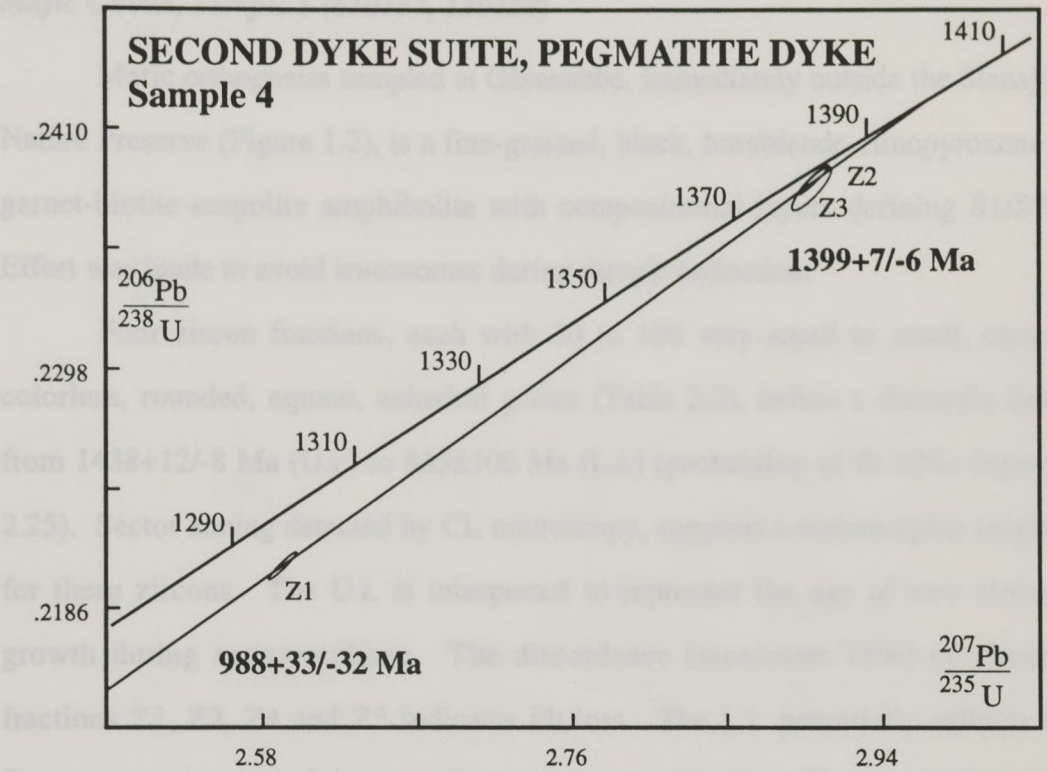

Figure 2.24. Concordia diagram for sample 4, zircon (Z). See text for discussion.

Mafic Gneiss, Sample 5 (630157, 130450)

Mafic orthogneiss sampled at Gåsanabbe, immediately outside the Stensjö Nature Preserve (Figure 1.2), is a fine-grained, black, hornblende-clinopyroxene-garnet-biotite-scapolite amphibolite with compositional layers defining S1/S2. Effort was made to avoid leucosomes during sample collection.

Four zircon fractions, each with 30 to 100 very-small to small, clear, colorless, rounded, equant, anhedral grains (Table 2.2), define a discordia line from 1438+12/-8 Ma (U.i.) to 855±100 Ma (L.i.) (probability of fit 22%; Figure 2.25). Sector zoning detected by CL microscopy, supports a metamorphic origin for these zircons. The U.i. is interpreted to represent the age of new zircon growth during metamorphism. The discordance (maximum 18%) of zircon fractions Z1, Z2, Z4 and Z5 indicates Pb loss. The L.i. potentially reflects a Sveconorwegian age, but may also represent multi-stage Pb loss during the Sveconorwegian Orogeny and again more recently.

Two fractions of very-large (>100 μm), clear, dark brown to light yellow, anhedral, rounded and fragmented titanite yield a concordant age of 935±5 Ma (Figure 2.25, inset), constraining more tightly the age of Sveconorwegian metamorphism.

Pegmatite Dyke, Third Dyke Suite, Sample 6 (630080, 130509)

Sample 6, collected in the Stensjö Nature Preserve (Figure 1.2), belongs to the third dyke suite. It escaped ductile deformation, but it is brittlely tectonized, with kinked biotites. Very large (1-5 mm), inclusion-rich, euhedral zircons

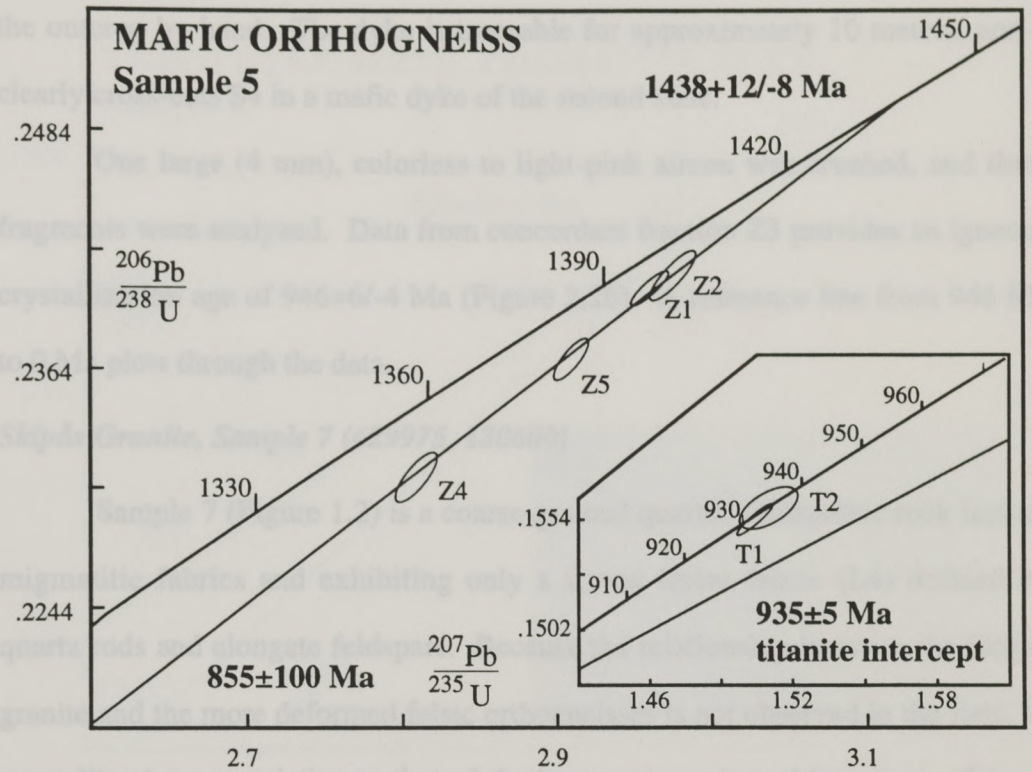

Figure 2.25. Concordia diagram for sample 5, zircon (Z) and titanite (T; inset). See text for discussion.

(Figure 2.26, inset) from this quartzo-feldspathic pegmatite were extracted from the outcrop by hand. The dyke is traceable for approximately 10 meters, and it clearly cross-cuts S4 in a mafic dyke of the second suite.

One large (4 mm), colorless to light-pink zircon was crushed, and three fragments were analyzed. Data from concordant fraction Z3 provides an igneous crystallization age of 946+6/-4 Ma (Figure 2.26). A reference line from 946 Ma to 0 Ma plots through the data.

Skipås Granite, Sample 7 (629975, 130600)

Sample 7 (Figure 1.2) is a coarse-grained quartzo-feldspathic rock lacking migmatitic fabrics and exhibiting only a strong linear fabric (L4) defined by quartz rods and elongate feldspars. Because the relationship between the Skipås granite and the more deformed felsic orthogneisses is not observed in the field, its crystallization age relative to that of the host gneisses is problematical. Zircons with a wide range of morphologies were extracted, including small to large, clear to inclusion-rich and/or highly fractured, colorless to light yellow, anhedral to euhedral, equant to elongate grains. Some crystals contain obvious cores. Four zircon fractions comprising small to medium, colorless, subhedral to euhedral grains with few inclusions were analyzed. The data points do not produce a well-defined discordia line (Figure 2.27), the $^{207}Pb/^{206}Pb$ ages for the four fractions ranging from 1582 Ma to 1656 Ma.

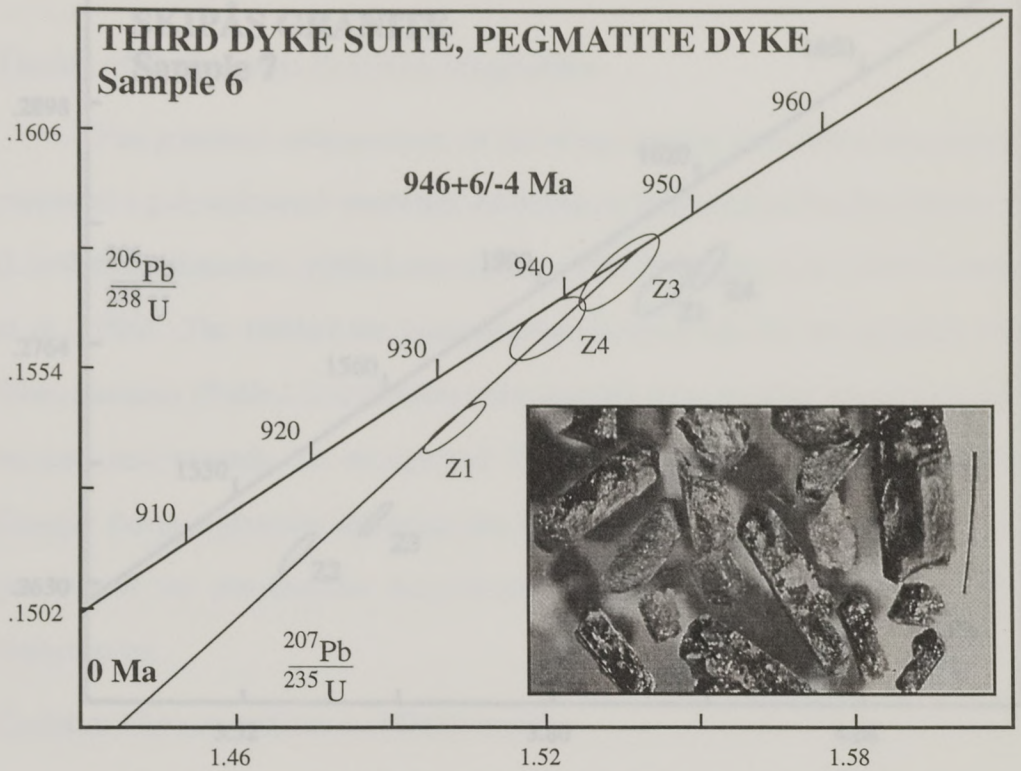

Figure 2.26. Concordia diagram for sample 6, zircon (Z). The inset shows grains similar to the analysed grain. The wire at the right is ~1 cm in length. See text for discussion.

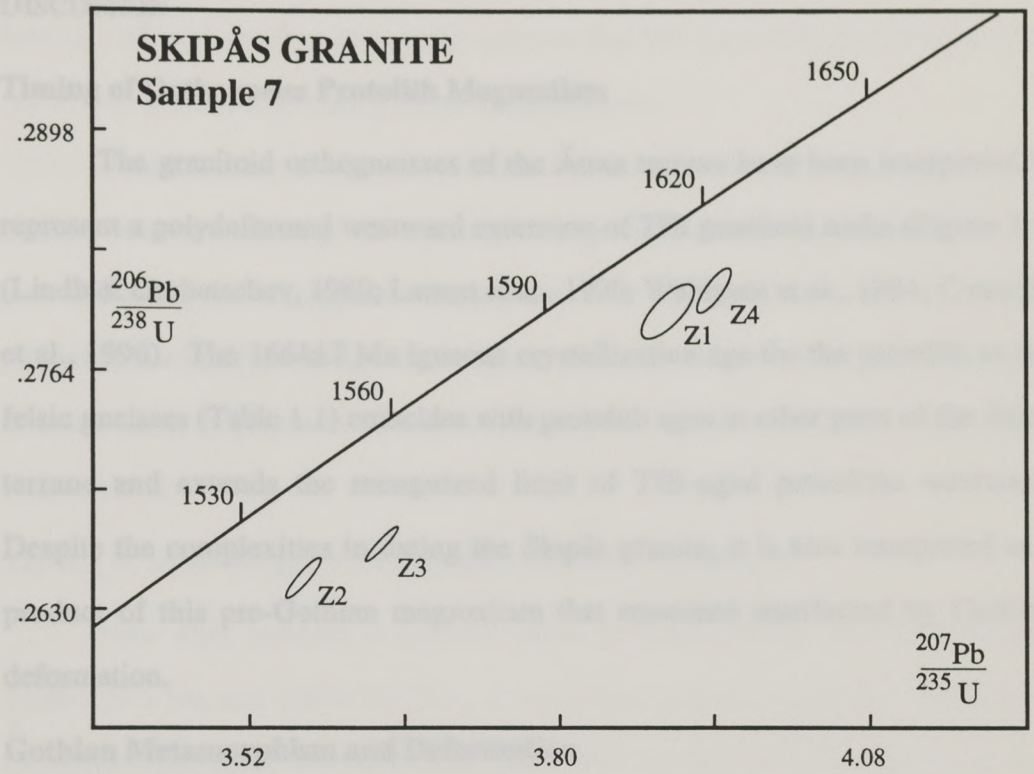

Figure 2.27. Concordia diagram for sample 7, zircon (Z). See text for discussion.

DISCUSSION

Timing of Orthogneiss Protolith Magmatism

The granitoid orthogneisses of the Ätran terrane have been interpreted to represent a polydeformed westward extension of TIB granitoid rocks (Figure 1.1) (Lindh & Gorbatschev, 1980; Larson et al., 1990; Wahlgren et al., 1994; Connelly et al., 1996). The 1664±7 Ma igneous crystallization age for the protolith to the felsic gneisses (Table 1.1) coincides with protolith ages in other parts of the Ätran terrane and extends the recognized limit of TIB-aged protoliths westward. Despite the complexities in dating the Skipås granite, it is also interpreted as a product of this pre-Gothian magmatism that remained unaffected by Gothian deformation.

Gothian Metamorphism and Deformation

Slight obliquity between the first dyke suite and S1 of the orthogneisses (Figure 1.15) suggests that D1 and the first event of migmatization preceded emplacement of the first dyke suite. According to zircon data, the first dyke suite was metamorphosed at 1654±9 Ma and was emplaced between 1664±7 Ma and 1654±9 Ma (Table 1.1), at an age indistinguishable from the age of the orthogneiss protolith and formation of S1 and N1. D1 and its associated migmatization must therefore be assigned to the Gothian Orogeny.

N2 formed during post-D1 metamorphism and cross-cuts N1 and S1. This metamorphism is assumed to correspond to metamorphic zircon growth in the first dyke suite (sample 2). Thus, N2 is interpreted to have formed

contemporaneously with the zircon at 1654±9 Ma (Table 1.1). Field relationships between N2 and the first dyke suite indicate that N2 formed during D2; thus D2 occured at 1654±9 Ma, during the Gothian Orogeny.

Determination of Gothian P-T conditions is precluded by high-grade post-Gothian recrystallization. Gothian-aged migmatization in mafic rocks suggest that metamorphic conditions during D1 and D2 were at least at upper-amphibolite-facies given that the temperatures required to induce partial melting in mafic rocks is greater than 650°C (Clemens & Vielzeuf, 1987; Sawyer, 1991; Peacock et al., 1994).

Timing of Inter-orogenic Magmatism and Metamorphism

New data indicate a thermal event in southwestern Sweden between 1438+12/-8 Ma and 1399+7/-6 Ma. It coincides with the suggested "Hallandian Orogeny" (Hubbard, 1975); whether there was associated deformation remains unknown.

Igneous crystallization ages 1426+9/-4 Ma and 1399+7/-6 Ma from pegmatite samples 3 and 4 represent the local maximum and minimum ages for the magmatic component of the thermal event (Table 1.1). Large charnockites to the north yield ages of *ca.* 1.4 Ga (Åhäll et al., 1992; Åhäll et al., 1997a), indicating that magmatism was regional. Neither the charnockites nor the *ca.* 1.4 Ga dykes in the Falkenberg-Halmstad area were subsequently migmatized (Åhäll, 1996), although the dykes themselves may be products of migmatization. If so, this could account for local occurrences of N3 leucosomes (Figure 1.5).

We now have definite evidence that metamorphic recrystallization was coeval with the inter-orogenic magmatism, supported by evidence for new zircon growth in the mafic gneiss (sample 5) at 1438+12/-8 Ma, during amphibolite- to upper-amphibolite-facies metamorphism.

An interesting observation is that the sampled mafic gneiss yields a younger metamorphic age (1438+12/-8 Ma) than the mafic dyke of the first suite (1654±9 Ma), given that both must have been present at *ca.* 1.65 Ga. This difference in timing of zircon growth may be linked to the breakdown of orthopyroxene that may have been controlled by 1) compositional differences between the two rocks, 2) different points in P-T space, and/or 3) differences in the activity of H_2O.

Timing of D3

As discussed above, F3 folds are refolded by F4 folds. This constrains the timing of D3 to between 1654±9 Ma, the age of D2, and 1426+9/-4 Ma, the maximum age for D4 (discussed below) (Table 1.1). Thus, D3 most likely occurred during the Gothian Orogeny.

Timing of Sveconorwegian Effects

D4 must have occurred between the crystallization age of pegmatite sample 3 (*ca.* 1.4 Ga) and the crystallization age of the post-D5, undeformed pegmatite sample 6 (*ca.* 0.94 Ga) (Table 1.1). Deformation associated with the *ca.* 1.4 Ga "Hallandian" thermal event can not be ruled out. Poorly known timing of deformation of the second dyke suite must be post-Gothian. We interpret the

timing of D4 to be Sveconorwegian, the only locally and regionally known, post-1426 Ma event.

Earlier isotope studies of the Sveconorwegian Orogeny in southwestern Sweden (Johansson et al., 1991; Johansson & Johansson, 1993; Cornell et al., 1996; Page et al., 1996; Söderlund, 1996; Wang et al., 1997) have pointed to a 990 to 900 Ma age for Sveconorwegian upper-amphibolite- to granulite-facies metamorphism, consistent with metamorphism in the Falkenberg-Halmstad area between 988+33/-32 Ma (Pb loss from pegmatite sample 3 zircons) and 932±7 Ma (recrystallization of titanite in sample 1). Three other Sveconorwegian metamorphic ages from the study fall between within this range. In spite of well-documented granulite-facies conditions, Sveconorwegian metamorphism did not cause partial melting, probably due to earlier dehydration during the Gothian Orogeny. Pervasive static recrystallization textures, also noted by Johansson et al. (1996) elsewhere in the Ätran terrane, developed during the Sveconorwegian orogeny (Figures 1.7 & 1.20).

Closure temperatures for retention of Pb in monazite, titanite and rutile bear upon the history of cooling at the end of the Sveconorwegian Orogeny. These are estimated to be 720°C for monazite (Copeland et al., 1988; Parrish, 1990; Mezger et al., 1991), 550°-650°C for titanite (Gascoyne, 1986; Tucker et al., 1987; Heaman & Parrish, 1991; Mezger et al., 1991; Mezger et al., 1993) and 380°-420°C for rutile (Mezger et al., 1989), leading to calculated cooling rates of 4.5-11°C/million years between 948 Ma and 932 Ma, and 2.5-5°C/million years between 932 Ma and 878 Ma, depending upon choice of closure temperatures. As shown by Mezger et al. (1991) for the Adirondacks, such slow cooling rates

indicate slow (passive?) exhumation of the Ätran terrane, possibly driven by erosion and collapse of the Sveconorwegian Orogen. In other parts of the world, such as Taiwan and the Himalayas, rapid cooling rates of 70°-460°C/million years are attributed to large-scale, active extensional and contractional tectonic processes (Liu, 1982; Foster et al., 1994; Adriessen & Zeck, 1996; Chen et al., 1996).

SUMMARY

Field relationships and U-Pb ages constrain the timing of Mesoproterozoic magmatism, metamorphism and deformation in southwestern Sweden between Falkenberg and Halmstad. The 1664±7 Ma felsic gneiss protolith age (sample 1) extends the known area for coeval magmatism in the TIB and the Ätran terrane farther west than previously recognized. This age and the metamorphic age of the mafic dyke (sample 2) constrain the emplacement age of the first dyke suite and the timing of the first migmatization (N1) and D1 deformation to between 1664±7 Ma and 1654±9 Ma, during the Gothian Orogeny. Metamorphism, migmatization (N2) and D2 deformation of the orthogneisses and the first dyke suite occurred at 1654±9 Ma. D3 is constrained to between 1654±9 Ma and 1426+9/-4 Ma, suggesting that D1-D3 were all a result of the Gothian Orogeny.

U-Pb zircon crystallization ages for the sample 3 (1426+9/-4 Ma) and sample 4 (1399+7/-6 Ma) pegmatites, combined with previous data for the 1409±20 Ma Glassvik pegmatite by Söderlund (1996), indicate that local magmatism occurred at *ca.* 1.4 Ga. More importantly, the 1438+12/-8 Ma metamorphic zircon age obtained for the Gothian-derived mafic gneiss is the first

evidence reported for metamorphism at this time in southwestern Sweden. Both magmatism and metamorphism between 1438+12/-8 Ma and 1399+7/-6 Ma indicate high heat flow and thus represent a regional thermal event. This thermal event supports previous suggestions of a high-temperature "Hallandian" metamorphic event. Deformation associated with this thermal event has not been demonstrated.

The crystallization age of the undeformed pegmatite constrains the end of D4 deformation locally to between 1426+9/-4 Ma and 946+6/-4 Ma, but a Sveconorwegian age is favored. As determined by field relationships and geochronology, the main gneiss-forming event in the study area occurred during the Gothian Orogeny. In comparison, local Sveconorwegian deformation effects are subordinate.

Static recrystallization textures indicate that metamorphism persisted after deformation ceased. Metamorphic monazite (948±4 Ma), titanite (932±7 Ma and 935±5 Ma) and rutile (878±10 Ma) also indicate that temperatures in the study area remained high until at least 878±10 Ma. The progressive younging of these mineral ages combined with their closure temperatures reflect slow cooling rates during isostatic unroofing of the Sveconorwegian Orogen.

Appendix A: Mineral Assemblages

SAMPLE	MINERALS																				
	plag	qtz	kspar	bio	amph	cpx	opx	epid	scap	gt	musc	zirc	tit	op	ap	chl	ru	ser	mon	tour	cc
Felsic Orthogneisses																					
95-1A	X	X	X	X							X	X		X	X			X			
95-18	X	X	X	X								X		X		X		X			
95-47	X	X	X	X	X					X		X		X	X	X		X			
95-56A	X	X	X	X							X										
95-63A	X	X		X	X					X		X		X		X		X			
95-65	X	X	X	X	X							X		X	X			X			
G95-79A: sample 1	X	X	X	X	X						X	X		X	X			X			X
Skipås Granite																					
95-26	X	X		X	X					X				X				X			
G95-39A: sample 7	X	X	X	X	X					X		X		X	X	X		X			
Mafic Orthogneisses																					
95-1B	X	X		X	X					X		X		X	X						
95-13F	X			X	X					X				X				X			X
G95-13G	X	X		X	X	X				X	X	X		X	X	X		X			X
G95-13H: sample 5	X	X		X	X	X			X	X		X	X	X	X			X			
95-14B	X			X	X					X				X				X			
95-23	X	X		X	X					X		X		X				X			
95-54	X			X	X	X			X	X											
95-81A	X	X		X	X	X				X		X	X	X				X			
95-81B	X	X		X	X	X	X			X		X	X	X	X						
Mafic Dykes, First Dyke Suite																					
95-13C	X				X	X			X	X		X		X		X		X			
95-13E	X			X	X				X	X		X	X					X			
G95-39B	X			X	X	X				X		X			X	X					

95-63B	X			X	X	X									X			X			
G95-79B: sample 2	X				X	X						X		X	X	X		X			X
Felsic Dykes, Second Dyke Suite																					
G95-79C: sample 3	X	X	X	X							X	X		X		X	X	X	X		
Mafic Dykes, Second Dyke Suite																					
G95-4B	X	X		X	X							X	X	X	X			X			
95-5B	X			X	X					X		X		X	X			X			
95-9A	X			X	X	X				X		X		X	X						X
95-9B	X			X	X	X				X			X	X	X	X					X
95-13A	X			X	X	X				X				X	X	X					
95-13B	X			X	X	X				X							X				
95-13D	X			X	X				X	X				X	X			X			
Pegmatite, Third Dyke Suite																					
G95-4A: sample 6	X	X	X								X	X									
Mafic Dykes, Third Dyke Suite																					
95-5A	X	X		X	X			X		X				X	X	X					
G95-66	X			X	X			X		X			X	X							

Sample numbers in bold are geochronology samples.

X indicates that the mineral is present.

Appendix B: U-Pb Techniques

Seven approximately 10 kg samples for geochronology were crushed, and standard mineral separation techniques were employed at the University of Texas at Austin to obtain mineral separates of zircon, titanite, monazite and rutile.

U-Pb analyses were performed at the University of Texas at Austin. Separated mineral fractions were carefully picked and selected based on optical properties using binocular and petrographic microscopes and morphological distinctions upon the basis of cathodoluminescence (CL) microscopy (Appendix C). Grains with inclusions and fractures, identified optically, were eliminated. Masses of analyzed fractions ranged from 2 μg to 181 μg.

All fractions were air-abraded using the technique of Krogh (1982), then re-examined and cleaned with distilled 4N nitric acid, quartz-distilled water and distilled acetone. Grains were weighed into Teflon® dissolution bombs with a mixed $^{205}Pb/^{235}U$ isotopic tracer and dissolved with HF and HNO_3 acids. For zircon analysis, U and Pb chemical separation was accomplished using minicolumns (100 μl resin volume) following the procedure of Krogh (1973). Pb blanks were 1-2 picograms. For titanite analysis, HBr chemistry was employed using 120 μl columns with a procedural blank of 2-3 picograms. U and Pb were loaded together onto outgassed, zone-refined rhenium filaments using silica gel and phosphoric acid.

Isotopic analyses were performed on a Finnigan MAT 261 thermal ionization mass spectrometer in static and/or peak jumping mode depending on

sample size and Pb concentrations. In the peak jumping mode, ^{204}Pb was measured in the axial secondary electron multiplier (SEM)/ion counter.

Ages were calculated using an unpublished program written by J. Connelly incorporating decay constants of Jaffey et al. (1971). Analytical errors of isotope ratios, reported at two sigma, were calculated with a program modified by J. Connelly after an unpublished error propagation program written by L. Heaman (Royal Ontario Museum, Toronto, Canada). Linear regressions were calculated using the procedure of Davis (1982); an acceptable probability of fit is 10%, corresponding to an MSWD of 2.

Appendix C: Cathodoluminescence Techniques

Zircons of different morphologies were selected to characterize their origin as igneous or metamorphic. Grains were mounted in epoxy and polished to their central sections. Analyses were performed at the University of Texas at Austin on a JEOL scanning electron microscope equipped to observe cathodoluminesence, by which variations in intensity of the luminescence reveals growth patterns.

References

Åhäll, K-I., Daly, J.S. & Schöberg, H., 1990. Geochronological constraints on Mid-Proterozoic magmatism in the Östfold-Marstrand belt: implications for crustal evolution, SW Sweden. In Gower, C.F., Rivers, T., & Ryan, B. (eds.): Mid-Proterozoic Laurentia-Baltica. *Geological Association of Canada Special Paper 38*: 97-115.

Åhäll, K-I., Samuelsson, L. & Persson, P-O., 1992. The age of the Torpa granite and its implications for the metamorphism in the Varberg region, SW Sweden. *Geologiska Föreningens i Stockholm Förhandlingar*, 114: 449-450.

Åhäll, K-I., Connelly, J.N., Samuelsson, L., Brewer, T.S., Daly, J.S. & Larson, S.Å., 1993. New age constraints for crustal growth and anorogenic evolution, SW Sweden. Symposium on "the Svecofennian Domain" and annual meeting of IGCP-275. Turku, Finland, August 23-25, 1993. Abstracts.

Åhäll, K-I., 1995. Crustal units and role of the Mylonite Zone system in the Varberg-Horred region, SW Sweden. *Geologiska Föreningens i Stockholm Förhandlingar*, 117: 185-198.

Åhäll, K-I., 1996. Interpreting the history of the southern part of the Eastern Segment, the Sveconorwegian Orogen of southwestern Sweden: A reply. *Geologiska Föreningens i Stockholm Förhandlingar*, 118: 189-192.

Åhäll, K-I. & Gower, C.F., 1997. The Gothian and Labradorian orogens: Variations in accretionary tectonism along a late Paleoproterozoic Laurentia-Baltica margin. *Geologiska Föreningens i Stockholm Förhandlingar*, 119: 181-191.

Åhäll, K-I., Samuelsson, L. & Persson, P-O., 1997a. Geochronology and structural setting of the 1.38 Ga Torpa granite; implications for charnockite formation in SW Sweden. *Geologiska Föreningens i Stockholm Förhandlingar*, 119: 37-43.

Åhäll, K-I., Connelly, J.N., Christoffel, C.A., & Larson, S. Å, 1997b. Evidence for a penetrative regional Gothian gneiss-forming event in the granulite area of the southern Sveconorwegian orogen, SW Sweden. *Geologiska Föreningens i Stockholm Förhandlingar*, 119: 192.

Åhäll, K-I. & Connelly, J.N., in press. Intermittent 1.51-1.15 Ga anorogenic magmatism in SW Sweden: Age constraints and correlations within Laurentia-Baltica. *Precambrian Research.*

Adriessen, P.A.M. & Zeck, H.P., 1996. Fission-track constraints on timing of Alpine nappe emplacement and rates of cooling and exhumation, Torrox area, Beltic Cordilleras, S. Spain. *Chemical Geology,* 131: 199-206.

Andersson, J., 1996. Sveconorwegian influence on the ca. 1.36 Ga old Tjarnesjo granite, and associated pyroxene-bearing quartz-monzonites in southwestern Sweden. *Geologiska Föreningens i Stockholm Förhandlingar*, 118, Jubilee Issue: A7-A8.

Berglund, J. & Connelly, J.N., 1994. The Vårgårda intrusion: Tectonic setting, age and regional implication. *Abstract volume, 21: a geologiska vintermötet i Luleå.*

Berglund, J., 1997. Compressional and extensional ductile shearing along a terrane boundary in south-western Sweden. In Berglund, J.: Mid-Proterozoic Evolution in South-Western Sweden. Ph.D. thesis, Lund, 1997.

Berthelsen, A., 1980. Towards a palinspastic tectonic analysis of the Baltic Shield, *in* Geology of Europe from Precambrian to the post-Hercynian sedimentary basins. International Geological Congress, Colloquium C6, Paris: 5-20.

Chen, C-H., DePaolo, D.J. & Lan, C-Y., 1996. Rb-Sr microchrons in the Manaslu granite: Implications for Himalayan thermochronology. *Earth and Planetary Science Letters*, 143: 125-135.

Clemens, J.D. & Vielzeuf, D., 1987. Constraints on melting and magma production in the crust. *Earth and Planetary Science Letters*, 86: 287-306.

Connelly, J.N. & Åhäll, K-I., 1996. The mid-Proterozoic cratonisation of Laurentia-Baltica; new age constraints from SW Sweden. In Brewer, T.S., (ed.), Precambrian Crustal Evolution in the North Atlantic Region. *Geological Society Special Publication No. 112*: 261-273.

Connelly, J.N., Berglund, J. & Larson, S.Å., 1996. Thermotectonic evolution of the Eastern Segment of SW Sweden; tectonic constraints from U-Pb geochronology. In Brewer, T.S., (ed.), Precambrian Crustal Evolution in

the North Atlantic Region. *Geological Society Special Publication No. 112*: 297-313.

Copeland, P., Parrish, R.R. & Harrison, T.M., 1988. Identification of inherited radiogenic Pb in monazite and its implications for U-Pb systematics. *Nature*, 333: 760-763.

Cornell, D.H., Larson, S.Å., Berglund, J., Connelly, J.N., Armstrong, R., Nesbitt, B. & Milton, A., 1996. Genesis and U-Pb dating of zircon rims in migmatite. 22nd Nordic Geological Winter Meeting. Abo Akademi, Turku, Finland, January 8-11, 1996, Abstracts: 32.

Davis, D.W., 1982. Optimum linear regression and error estimation applied to U-Pb data. *Canadian Journal of Earth Science*, 23: 2141-2149.

Deer, W.A., Howie, R.A. & Zussman, J., 1992. *An Introduction to the Rock-Forming Minerals,* 2nd edition. Longman Scientific & Technical, Essex, England, 696 pp.

Foster, D.A., Gleadow, A.J.W. & Mortimer, G., 1994. Rapid Pliocene exhumation in the Karakoram (Pakistan), revealed by fission track thermochronology of the K2 gneiss. *Geology*, 22: 19-22.

Gaál, G. & Gorbatschev, R., 1987. An outline of the Precambrian evolution of the Baltic Shield. *Precambrian Research*, 35: 15-52.

Gascoyne, M., 1986. Evidence for the stability of the potential nuclear waste host, sphene, over geological time, from uranium-lead ages and uranium-series measurements. *Applied Geochemistry*, 1: 199-210.

Gorbatschev, R., 1980. The Precambrian development of southern Sweden. *Contributions to Mineralogy and Petrology*, 102: 129-136.

Gorbatschev, R., Lindh, A., Solyom, Z., Laitakari, I., Aro, K., Lobach-Zhuchenko, S.B., Markov, M.S., Ivliev, A.I. & Bryhni, I., 1987. Mafic dyke swarms of the Baltic Shield. *Geological Association of Canada Special Paper 34*: 361-372.

Gower, C.F., 1985. Correlations Between the Grenville Province and Sveconorwegian Orogenic Belt - Implications for Proterozoic Evolution of the Southern Margins of the Canadian and Baltic Shields. In Tobi A.C. & Touret J.L.R. (eds.) The Deep Proterozoic Crust in the Northern Atlantic Provinces: 247-257.

Gower, C.F., 1990. Mid-Proterozoic evolution of the eastern Grenville Province, Canada. *Geologiska Föreningens i Stockholm Förhandlingar*, 112: 127-139.

Gower, C.F., Ryan, A.B. & Rivers, T., 1990. Mid-Proterozoic Laurentia-Baltica: An overview of its geological evolution and a summary of the contributions made by this volume. In Gower, C.F., Rivers, T. & Ryan, A.B. (eds.) *Mid-Proterozoic Laurentia-Baltica*. Geological Association of Canada, Special Paper 38: 1-20.

Harley, S.L., 1989. The Origin of Granulites: A metamorphic perspective. *Geological Magazine*, 126: 215-247.

Heaman, L. & Parrish, R., 1991. U-Pb geochronology of accessory minerals. in Heaman, L. & Ludden, J.N. (eds.) *Applications of radiogenic isotope systems to problems in geology*, Short course handbook 19. Mineralogic Association of Canada, Toronto: 59-102.

Hoffman, P.F., 1992. Did the breakup of Laurentia turn Gondwanaland inside-out? *Science* , 252: 1409-1411.

Hubbard, F.H., 1975. The Precambrian crystalline complex of SW Sweden. The geology and petrogenetic development of the Varberg Region. *Geologiska Föreningens i Stockholm Förhandlingar*, 97: 223-236.

Hubbard, F. H., 1976. The Precambrian crystalline complex of SW Sweden, The geology and petrogenetic development of the Varberg Region. A reply. *Geologiska Foreningen i Stockholm Fohandlingar* , 98: 171-174.

Jaffey, A.H., Flynn, K.F., Glendenin, L.E., Bentley, W.C. & Essling, A.M., 1971. Precision measurements of half-lives and specific activities of ^{235}U and ^{238}U. *Physics Review,* C4: 1889-1906.

Jagoutz, E., 1988. Nd and Sr systematics in an eclogite xenolith from Tanzania: Evidence for frozen mineral equilibria in the continental lithosphere. *Geochimica et Cosmochimica Acta*, 52: 1285-1293.

Johansson, L., Lindh, A. & Möller, C., 1991. Late Sveconorwegian (Grenville) high-pressure granulite facies metamorphism in southwest Sweden. *Journal of Metamorphic Geology*, 9: 283-292.

Johansson, L. & Johansson, Å., 1993. U-Pb age of titanite in the Mylonite Zone, southwestern Sweden. *Geologiska Föreningens i Stockholm Förhandlingar*, 115: 1-7.

Johansson, L. & Kullerud, L., 1993. Late Sveconorwegian metamorphism and deformation in southwestern Sweden. *Precambrian Research*, 64: 347-360.

Johansson, L., Möller, C., Söderlund, U., Lindh, A. & Wang, X-D., 1996. Interpreting the history of the southern part of the Eastern Segment, the Sveconorwegian Orogen of southwestern Sweden: A discussion. *Geologiska Föreningens i Stockholm Förhandlingar*, 118: 187-189.

Kretz, R., 1983. Symbols for rock-forming minerals. *American Mineralogist*, 68: 277-279.

Krogh, T.E., 1982. Improved accuracy of U-Pb zircon ages by the creation of more concordant systems using an abrasion technique. *Geochimica et Cosmochimica Acta*, 46: 637-649.

Krogh, T.E., 1973. A low-contamination method for hydrothermal decomposition of zircon and extraction of U and Pb for isotopic age determinations, *Geochimica et Cosmochimica Acta*, 37: 485-494.

Larson, S.Å., Stigh, J. & Tullborg, E-L., 1986. The deformation history of the eastern part of the Southwest Swedish gneiss belt. *Precambrian Research*, 31: 237-257.

Larson, S.Å., Berglund, J., Stigh, J. & Tullborg, E-L., 1990. The Protogine Zone, southwest Sweden: A new model - an old issue. In Gower, C.F., Rivers, T. & Ryan, A.B. (eds.) *Mid-Proterozoic Laurentia-Baltica.* Geological Association of Canada, Special Paper 38: 317-333.

Larson, S.Å. & Berglund, J., 1992. A chronological subdivision of the Transscandinavian Igneous Belt - three magmatic episodes. *Geologiska Föreningens i Stockholm Förhandlingar*, 114: 459-461.

Larson, S.Å., 1996. The Gothian and Sveconorwegian terranes of SW Sweden. *Geologiska Föreningens i Stockholm Förhandlingar*, 118, Jubilee Issue: A17.

Lindh, 1996. The age of the Hinneryd granite - its significance for interpreting the terranes of the southern Baltic Shield. *Geologiska Föreningens i Stockholm Förhandlingar*, 118: 163-168.

Lindh, A. & Gorbatchev, R., 1980. Chemical variation in a Proterozoic suite of granitoids extending across a mobile belt-craton boundary. *Geologische Rundschau*, 73: 881-893.

Liu, T-K., 1982. Tectonic implication of fission track ages from the Central Range, Taiwan. *Proceedings of the Geological Society of China*, 25: 22-37.

Lundqvist, I., Larson, S.Å., Connelly, J.N. & Brewer, T.S., 1992. Midproterozoic intracontinental extension - evidence from an E-W trending, composite dyke swarm, south-central Sweden. *Abstract I.G.C.P. 257 Precambrian dyke swarms.* Petrozavodsk, Russia, Sept. 7-17: 51-52.

Machado, N., Goulet, N. & Gariépy, C., 1989. U-Pb geochronology of reactivated Archean basement and of Hudsonian metamorphism in the northern Labrador Trough. *Canadian Journal of Earth Science*, 26: 1-15.

Mattinson, J.M., 1978. Age, origin and thermal histories of some plutonic rocks from the Salinian Block of California. *Contributions to Mineralogy and Petrology*, 67: 233-245.

Mezger, K., Hanson, G.N. & Bohlen, S.R., 1989. High-precision U-Pb ages of metamorphic rutile: Application to the cooling history of high-grade terranes. *Earth and Planetary Science Letters*, 96: 106-118.

Mezger, K., Rawnsley, C.M., Bohlen, S.R. & Hanson, G.N., 1991. U-Pb garnet, sphene, monazite, and rutile ages; implications for the duration of high-grade metamorphism and cooling histories, Adirondack Mountains New York. *Journal of Geology*, v. 99: 415-428.

Mezger, K., Essene, E.J., van der Pluijm, B.A. & Halliday A.N., 1993. U-Pb geochronology of the Grenville Orogen of Ontario and New York: Constraints on ancient crustal tectonics. *Contributions to Mineralogy and Petrology*, 114: 13-26.

Möller, C. & Söderlund, U., 1996. Sveconorwegian metamorphism, deformation and age constraints of rocks in the Ullared area, Eastern Segment of SW Sweden. *Geologiska Föreningens i Stockholm Förhandlingar*, 118, Jubilee Issue: A21.

Möller, C. & Söderlund, U., 1997. Age constraints on the regional deformation within the Eastern Segment, S. Sweden: Late Sveconorwegian granite dyke intrusion and metamorphic-deformational relations. *Geologiska Föreningens i Stockholm Förhandlingar*, 119: 1-12.

Page, L., Möller, C. & Johansson, L., 1996. Ar/Ar geochronology across the Mylonite Zone and the Southwestern Granulite Province in the Sveconorwegian Orogen of S Sweden. *Precambrian Research*, 79: 239-259.

Park, R.G., Åhäll, K.-I., Crane, A. & Daly, S., 1987. The structure and kinematic evolution of the Lysekil-Marstrand area, Östfold-Marstrand Belt, southwestern Sweden. *Sveriges Geologiska Underökning*, C 816: 1-42.

Park, R.G., Åhäll, K.-I. & Boland, M.P., 1991. The Sveconorwegian shear-zone network of SW Sweden in relation to mid-Proterozoic plate movements. *Precambrian Research*, v.49: 245-260.

Parrish, R.R., 1990. U-Pb dating of monazite and its application to geological problems. *Canadian Journal of Earth Sciences*, 27: 1431-1450.

Peacock, S.M., Rushmer, T. & Thompson, A.B., 1994. Partial melting of subducting oceanic crust. *Earth and Planetary Science Letters*, 121: 227-244.

Persson & Wikström, 1993. A U-Pb dating of the Askersund granite and its marginal augen gneiss. *Geologiska Föreningens i Stockholm Förhandlingar*, 115: 321-329.

Quensel, 1951. The charnockite series of the Varberg district on the south-western coast of Sweden. *Arkiv för Mineralogi och Geologi*, v.1: 227-332.

Samuelsson, L. & Åhäll, K.-I., 1985. Proterozoic Development of Bohuslän, South-Western Sweden. In Tobi A.C. & Touret J.L.R. (eds.) The Deep Proterozoic Crust in the Northern Atlantic Provinces: 345-357.

Sawyer, E.W., 1991. Disequilibrium melting and the rate of melt-residuum separation during migmatization of mafic rocks from the Grenville Front, Quebec. *Journal of Petrology*, 32: 701-738.

Scott, D.J. & St-Onge, M.R., 1995. Constraints on Pb closure temperature in titanite based on rocks from the Ungava orogen, Canada: Implications for

U-Pb geochronology and P-T-t path determinations. *Geology*, 23: 1123-1126.

Söderlund, U., 1993. Structural and U-Pb isotopic age constraints on the tectonothermal evolution at Glassvik, Halland. Senior Thesis, Lund University, Lund, Sweden, 31 pp.

Söderlund, U., 1996. Conventional U-Pb dating versus single-grain Pb evaporation dating of complex zircons from a pegmatite in the high-grade gneisses of southwestern Sweden. *Lithos*, 38: 93-105.

Söderlund, U., Persson, P-O., Stephens, M.B. & Wahlgren, C-H., 1996. Zircon and titanite geochronology of gneissic granites in the Eastern Segment of the Sveconorwegian Orogen, southwestern Sweden. *Geologiska Föreningens i Stockholm Förhandlingar*, 118, Jubilee Issue: A26.

Stacey, J.C. & Kramers, J.D., 1975. Approximation of terrestrial lead isotope evolution by a two-stage model. *Earth and Planetary Science Letters,* 26: 207-221.

Starmer, I.C., 1991. The Proterozoic evolution of the Bamble sector shear belt, southern Norway: Correlations across southern Scandinavia and the Grenvillian controversy. *Precambrian Research*, 49: 107-139.

Talbot, C.J. & Heeroma, P., 1989. Cover/basement relationships in the SW Swedish gneisses near Varberg, *Geologiska Föreningens i Stockholm Förhandlingar*, 111: 105-119.

Tucker, R.D., Råheim, A., Krogh, T.E. & Corfu, F., 1987. Uranium-lead zircon and titanite ages from the northern portion of the Western Gneiss Region, south-central Norway. *Earth and Planetary Science Letters*, 81 p. 203-211.

Wahlgren, C-H., Cruden, A.R. & Stephens, M.B., 1994. Kinematics of a fan-like structure in the eastern part of the Sveconorwegian orogen, Baltic Shield, south-central Sweden. *Precambrian Research,* 70: 67-91.

Wang, X-D., Page, L.M. & Lindh, A., 1996. $^{40}Ar/^{39}Ar$ geochronological constraints from the southeasternmost part of the Eastern segment of the Sveconorwegian orogen: Implications for timing of granulite-facies metamorphism. *Geologiska Föreningens i Stockholm Förhandlingar*, 118: 1-8.

Wang, X-D., Söderlund, U., Lindh, A. & Johansson, L., 1997. U-Pb and Sm-Nd dating of high pressure granulite and upper amphibolite facies rocks from the southwest Swedish granulite region. In Wang, X-D.: Metamorphism and Geochronology of the High-Pressure Granulite and Upper Amphibolite Facies Rocks from the Southwest Swedish Granulite Region. Ph.D. thesis, Lund, 1996.

Welin, E., 1994. Isotopic investigations of Proterozoic igneous rocks in south-western Sweden. *Geologiska Föreningens i Stockholm Förhandlingar*, 116: 75-86.

Zhang, L-S. & Schärer, U., 1996. Inherited Pb components in magmatic titanite and their consequence for the interpretation of U-Pb ages. *Earth and Planetary Science Letters*, 138: 57-65.

The vita has been removed from the digitized version of this document.